THE PENNSYLVANIA STATE UNIVERSITY
SCHREYER HONORS COLLEGE

DEPARTMENT OF MECHANICAL AND NUCLEAR ENGINEERING

ON-SITE PERFORMANCE OF EXTENSIVE GREEN ROOFS

NICOLE L. PETERSON

Fall 2009

A thesis
submitted in partial fulfillment
of the requirements
for baccalaureate degrees
in Mechanical Engineering, Spanish, and International Studies
with honors in Mechanical Engineering

Reviewed and approved* by the following:

Jelena Srebric
Associate Professor of Architectural Engineering
Adjunct Professor of Mechanical Engineering
Thesis Supervisor

Matthew M. Mench
Associate Professor of Mechanical Engineering
Honors Advisor

*Signatures are on file in the Schreyer Honors College.

ABSTRACT

Green roofs are a sustainable technology that offers advantages over standard roofs, including benefits related to energy savings and drainage systems. This thesis focuses on the instrumentation and data analysis of extensive green roofs. A weather station—which will be implemented on the Forest Resources Building on the Pennsylvania State University's campus in the near future—has been designed. Then, through the analysis of measured variables collected on a green roof in Chicago, Illinois using similar instrumentation to that discussed in this thesis, it was determined that despite the benefits of green roofs, the white reflective standard roof performed better in terms of heat flux for summer conditions during July, 2007. In fact, the standard roof was shown to have savings of 309 $W \cdot hr/m^2 \cdot$month during the month analyzed. The data processing and analysis of the data will be used in the future for the validation of a new heat and mass transfer green roof model. Another analysis would need to be done to compare a green roof with a standard black roof. Future work may also deal with the properties of green roofs and the development of an inorganic-organic material that may have the same functions and benefits of a green roof.

TABLE OF CONTENTS

LIST OF FIGURES

LIST OF TABLES

ACKNOWLEDGEMENTS

First and foremost I would like to acknowledge Dr. Jelena Srebric, who thoughtfully guided me through this thesis project. She presented me with this opportunity and helped me find my direction within engineering as it relates to the environment. I cannot thank her enough and without her, this thesis would not have been possible. In the same regard, I would like to thank Paulo Cesar Tabares-Velasco, who dedicated his time to share his project with me. His knowledge and guidance has been invaluable. I am also grateful to my peers in the undergraduate research group. Weekly, they provided me with useful information and helpful ideas and suggestions. Thank you to Tyler Meek, Pavel Likhonin, Josh Wentz, and Adam Bernardo.

I would like to thank Dr. Matthew Mench for being my second reader and for serving as my Honors Adviser for the past three and a half years. His kind words and willingness to help have made all my brushes with the Penn State bureaucracy all the more easier. I am also forever indebted to Dr. Bo Kasal, who initially put me in touch with Dr. Srebric.

My friends know how grateful I am to them; whether at Penn State or elsewhere, my friends have provided me with an outlet throughout this thesis project and throughout college.

Last, but certainly not least, I would like to thank my family. My sister's undying faith in me has given me strength. My parents always taught me that I should not limit myself; that there is no "right" way of doing things and even when things do not go exactly as you planned, it is ok; that although it is important to work hard and be successful, life is not all about work; and finally, that I should always reach for my dreams, no matter how impossible it might seem.

Chapter 1

Introduction

This thesis will discuss extensive green roofs and their on-site performance. Much of the information will be based on research and experiments already performed over the past few years in the Architectural Engineering Laboratory, as well as data collected on a green roof in Chicago, Illinois. However, in order to move forward with this project, it is necessary to obtain more information with regard to the instrumentation that may measure various characteristics of the green roof. It is also important to analyze certain variables and view the performance of green roofs as compared with standard roofs.

1.1 Literature Review

Green roofs are defined as "specialized roofing systems that support plant growth on rooftops" (Liu et al., 2004). This sustainable technology is becoming very widespread as a solution for environmentally green building. At the Pennsylvania State University, this project was started by the Building Science Research Group. They built an Environmental Chamber, implemented a new and innovative apparatus named the "Cold Plate," and developed a heat and mass transfer model to describe a green roof.

Using the Environmental Chamber and "Cold Plate" apparatus, an experiment involving two setups—one with plants and one without—was performed. The plants used were *Sedum Spurium*. The experiment showed that plants do indeed maintain a vital role in the reduction of heat flux through a roof due to their ability to better manage latent heat flux and sensible heat

flux. In fact, a second experiment showed that plants are shown to reduce heat flux by 40-50%. In this experiment, there were three species: one without plants and one each with *Delosperma nubigenum* and *Sedum spurium*, both of which are considered drought tolerant species. Evapotranspiration is the combination of the evaporation of the substrate, or soil, and the transpiration of plants. It is a heat and mass transfer phenomena that is integral to the performance of green roofs. In this second experiment, evapotranspiration was measured using the lysimeter and water balance hydrological methods. It should be noted that these experiments were performed on extensive green roof samples. An extensive green roof differs from an intensive green roof in several respects; extensive green roofs are lighter, less expensive and require less maintenance than intensive green roofs. Extensive green roofs are more common than intensive green roofs in North America (Tabares-Velasco and Srebric, 2009c).

The following energy balance equation can be used to describe the heat transfer processes on a green roof (Tabares-Velasco and Srebric, 2009a):

$$R_n = ET + Q_{sensible} + Q_{conduction} + S_{thermal} + M$$

where

R_n = net radiation, equal to solar gain minus infrared heat losses, Btu/hr·ft^2 (W/m^2),

ET = evapotranspiration, or latent heat flux, Btu/hr·ft^2 (W/m^2),

$Q_{sensible}$ = convective or sensible heat flux, Btu/hr·ft^2 (W/m^2),

$Q_{conduction}$ = heat flux through roof, Btu/hr·ft^2 (W/m^2),

$S_{thermal}$ = thermal storage for substrate, plants, Btu/hr·ft^2 (W/m^2), and

M = metabolic storage (photosynthesis and respiration), Btu/hr·ft^2 (W/m^2).

This equation will be explained further and used for data analysis in Chapter 3.

Green roofs have been shown to have many advantages. Two of the main benefits are

related to drainage and peak energy savings. With regard to drainage, it should be noted that the soil and plants on a green roof absorb much of the rainfall, and thus, there is less runoff than there would be on a standard roof that does not have any medium to absorb the water. Secondly, in green roofs, the soil, along with processes such as evapotranspiration and shading, tends to decrease the load of the heat flux. This is significant in that the air conditioning in a building may be used less and, as a result, there may be great energy savings.

1.2 Motivation for On-Site Data Collection

While a heat and mass transfer model has already been developed, verified, and validated based on the green roof set up in the Environmental Chamber, further work must be completed on-site. The weather station designed in this thesis will be used by students in the future to collect data on the Forest Resources Building on campus. Once data is collected on this green roof, it may be applied to the model for further validation. The model was developed in the Environmental Chamber with steady state conditions, but by applying input data that was taken in a more realistic outdoor environment, the model will have an even stronger base. Additionally, the data from the green roof in Chicago may be processed and prepared for outdoor validation. The analysis of the data for the green roof in Chicago is significant, as there have been no previous studies comparing the performance of a green roof and a white reflective roof. This data analysis will give another perspective of the performance of green roofs as compared with another type of roof, illustrating its strengths and weaknesses. The data from the green roof in Chicago may ultimately be applied to the heat and mass transfer model for validation as well.

1.3 Outline of Remaining Chapters

The following chapters will follow the design process, data analysis, and validation of a model for green roofs. Chapter 2 will outline the process of designing a weather station. Subsequently, data collected from a previous study on a green roof in Chicago will be analyzed, and the results will be presented in Chapter 3. Finally, Chapter 4 will discuss the conclusions of this project, as well as future work.

Chapter 2

Weather Station Design

The initial task in this thesis project was to choose instruments from weather station manufacturers that provide the necessary data collection. The instruments may then be purchased and used in the experimental set-up for the green roof on campus. The process of choosing a manufacturer and its instruments essentially implements the idea of Design of Experiments.

2.1 Inputs

The inputs necessary for the existing heat and mass transfer model are: (1) air temperature, (2) air relative humidity, (3) air speed, (4) solar radiation, and (5) precipitation (Tabares-Velasco, 2009). Based on these parameters, several manufacturers could be considered. Table 2-1 outlines which manufacturers can potentially collect which inputs (MicroDAQ, 2009).

Table **2.1**: Weather Station Manufacturers and Available Inputs.

inputs	HOBO	WatchDog 2900ET	WatchDog 2700ET	WatchDog Mini	Davis
air temperature	✓	✓	✓	✓	✓
air relative humidity	✓	✓	✓	✓	✓
air speed	✓	✓	✓		
solar radiation	✓	✓			
precipitation	✓	✓	✓		✓

As seen in the table, models from Onset HOBO and the Spectrum Technologies' WatchDog Model 2900ET are the only ones that measure and record all of the inputs necessary for the green roof heat and mass transfer model. The other manufacturers may then be eliminated.

2.2 Tradeoffs and Accuracy

The next step is to look at the tradeoffs of cost and accuracy. If an instrument is too accurate, it may be too expensive; conversely, if an instrument is very cheap, it may be very inaccurate as well. In choosing equipment, it is important to find a balance when considering these tradeoffs for several reasons. The purpose of the instrument must be taken into account, as well as the budget.

The cost of each model of the Onset HOBO and WatchDog are shown in Table 2-2 (MicroDAQ, 2009).

Table **2.2**: Costs of Onset HOBO and WatchDog models.

	Onset HOBO			
	Micro Station Data Logger	Weather Station Data Logger	U30 Weather Station Starter Kit	Watchdog 2900ET
cost	$215	$460	$1,350	$1,695

It would appear that the Onset HOBO Micro Station Data Logger is the most cost effective. However, all of the Onset HOBO data loggers require HOBOWare Pro Software and data sensors, which would add to the cost. These data sensors differ in their specifications. The measurement range, accuracy of measurements, and cost—which is also dependent on the length of the cable included—of each Smart Sensor are outlined in Table 2-3 (MicroDAQ, 2009).

Table **2.3**: Onset HOBO Smart Sensor Specifications.

	Measurement Range	Accuracy	Cost
12-Bit Temperature Smart Sensor	-40°C to 100 °C (-40°F to 212°F)	< ±0.2°C from 0°C to 50°C (< ±0.36°F @ 32°C to 122°F)	$95 (with 2 m cable) $105 (with 6 m cable) $120 (with 17 m cable)
12-Bit Temp/RH Smart Sensor	Temperature: -40°C to 75°C (-40°F to 167°F) Humidity: 0 to 100% RH at -40°C to 75°C (-40°F to 167°F)	Temperature: 0.2°C @ 0°C to 50°C (±.36°F @ 32°C to 122°F) Humidity: ±2.5% from 10 to 90% RH	$185 (with 2 m cable) $195 (with 8 m cable)
Wind Speed Smart Sensor	0 to 45 m/s (0 to 100 mph)	±1.1 m/s (2.4 mph) or 4% of reading whichever is greater	$239 (with 3 m cable)
Wind Speed/Direction Smart Sensor	Wind speed gust: 0 to 44 m/s (0 to 99 mph) Wind direction: 0 to 358°, 2° Dead Band	Wind speed gust: ±0.5 m/s ±3% 17 to 30 m/s ±4% 30 to 47 m/s Wind direction: ±5 Degrees	$540 (with 3 m cable)
Silicon Pyranometer Smart Sensor	0 to 1280 W/m^2	±10.0 W/m^2 or ±5%, whichever is greater in sunlight. Additional temperature induced error 0.38 W/m2/°C from 25°C (0.21 W/m2/°F from 77°F)	$210 (with 3 m cable)
Rain Gauge Smart Sensor	10 cm or 0" to 5" per hour; maximum 4000 tips per interval	±1.0% at up to 20 mm or 1" per hour	$410

It should be noted that generally sensors have better accuracy when they are measuring separate data. For example, it would have been ideal to obtain two separate sensors, one for temperature and one for relative humidity, rather than a single sensor that measures both of these variables; however, there is no sensor available for relative humidity alone.

At a cost of $1,695, the WatchDog Model 2900ET has specifications for measurement range and accuracy as shown in Table 2-4 (MicroDAQ, 2009).

Table **2.4**: WatchDog Model 2900ET Specifications.

	Measurement Range	**Accuracy**
wind speed	0 to 175 mph	±5%
wind direction	2° Increments	±7°
temperature	-20°C to 70°C (-4°F to 158°F)	±0.6°C (±1.0°F)
relative humidity	20% to 100% @ 5°C to 50°C	±3%
rainfall	0.01" (0.25cm) Resolution	± 5%
solar radiation	1 to 1250 W/m^2	±5%

Finally, a waterproof heat flux meter for outdoor use must be purchased. Three models have been found to meet these criteria: The HFP01-L and HFP01SC-L Hukseflux Soil Heat Flux Plates manufactured by Campbell Scientific and the Model GHT-1C Geothermal Heat Flux Transducer manufactured by International Thermal Instrument Company. The specifications of these instruments are shown in Table 2.5 (International Thermal Instrument Company, 2008 and Campbell Scientific, 2009b).

Table **2.5**: Heat Flux Meter Specifications.

	HFP01-L	**HFP01SC-L**	**GHT-1C**
Sensor	Thermopile	Thermopile with film heater	Thermopile
Sensitivity	0.02 W/m^2·mV	0.02 W/m^2·mV	1.1 W/m^2·mV
Temperature Range	-30°C to +70°C	-30°C to +70°C	-37.7°F to +121°C
Accuracy	within -15% to +5% in most common soils	±3%	±1%
Dimensions	Plate thickness: 0.20” Plate Diameter: 3.15”	Plate thickness: 0.20” Plate Diameter: 3.15”	0.225” x 6” x 6.5”
Price	$635	$1,245	$625

From the table, it can be seen that the GHT-1C has a wider temperature range than the HFP01-L, as well as lower accuracy and higher sensitivity. In fact, according to an International Thermal Instrument Company representative contacted with regard to this sensor, the GHT-1C is “most sensitive sensor on the market.” The GHT-1C also provides information about its

response time, with a time constant of approximately 15 seconds. The prices of the GHT-1C and HFP01-L models are fairly similar, while the price for the HFP01SC-L is almost twice as high, likely because, as noted in the brochure, it "is intended for applications that do not require self-calibration" (Campbell Scientific, 2009b). However, since self-calibration is not required in this case, the GHT-1C seems to be the best option.

2.3 Conclusions

It seems that the best option would be to buy the Onset HOBO Micro Station Data Logger with the 12-Bit Temperature/Relative Humidity Smart Sensor (with the 8 meter cable), Wind Speed/Direction Smart Sensor, Silicon Pyranometer Smart Sensor, and Rain Gauge Smart Sensor. Purchasing this Data Logger with all Smart Sensors would cost $1,570. We may compare this to the cost of $1,695 for the WatchDog 2900ET model. The accuracy of the Onset HOBO Data Logger and the WatchDog 2900ET model may also be compared. The Onset HOBO Micro Station Data Logger is the most cost effective and will yield the most accurate results for the current green roof experimental setup. It also provides a greater measurement range for all parameters.

With regard to the heat flux meter, from the information in Table 2.5, it seems that the Model GHT-1C Geothermal Heat Flux Transducer manufactured by International Thermal Instrument Company is suitable for the purposes on this project and it will be purchased in the near future.

It should be noted that five moisture content sensors have already been purchased for the laboratory for the green roof. These sensors are CS616 Water Content Reflectometers by

Campbell Scientific (Campbell Scientific, 2009a). Additionally, a pyregeometer for measurements of sky radiation is already available. Sky radiation is an optional input for the heat and mass transfer model.

Typically in Design of Experiments, redesign is necessary. However, in this case, the Onset HOBO Micro Data Logger and the Smart Sensors chosen will surely be sufficient for the project on hand. As an alternative to immediate redesign, once the Weather Station is put into place on the green roof on campus, the results and satisfaction of the instrumentation will be analyzed and reported. Thus, in the future, more Smart Sensors and cables may be purchased to improve the Weather Station design.

Chapter 3

Data Analysis

The following information is based on data collected on a roof in Chicago during the month of July, 2007. The data was collected with a weather station similar to that discussed in Chapter 2. The roof was split into a green roof and a "standard" roof. It is important to note that with regard to this data, the "standard" roof is in fact a white reflective roof. It is hoped that this data may help apply the heat and mass transfer model developed by Dr. Srebric and Paulo Cesar Tabares-Velasco. The measured variables are as follows:

- Roof top wind speed (miles/hour)
- Standard roof radiation (W/m^2)
- Green roof radiation (W/m^2)
- Air temperature (°F)
- Relative humidity, RH (%)
- Precipitation (Rain tot, inches)
- Soil moisture
- Green roof surface temperature (°F)
- Standard roof surface temperature (°F)
- Soil temperature (°F)
- Solar radiation (W/m^2)
- Standard roof under membrane temperature 1 (°F)
- Standard roof under membrane temperature 2 (°F)
- Green roof under membrane temperature 1 (°F)
- Green roof under membrane temperature 2 (°F)
- Standard roof heat flux 1 (W/m^2)
- Standard roof heat flux 2 (W/m^2)
- Green roof heat flux 1 (W/m^2)
- Green roof heat flux 2 (W/m^2)

The analysis of this data is important in speculating whether or not a green roof has better performance than the standard roof, and examining what the differences between the two

roofs are. The following chapter contains an analysis of the measured variables, starting out with quality control and continuing with weekly plots of the data and a statistical analysis of the heat flux. The setup of the sensors used to measure the variables can be seen in Figure 3.1.

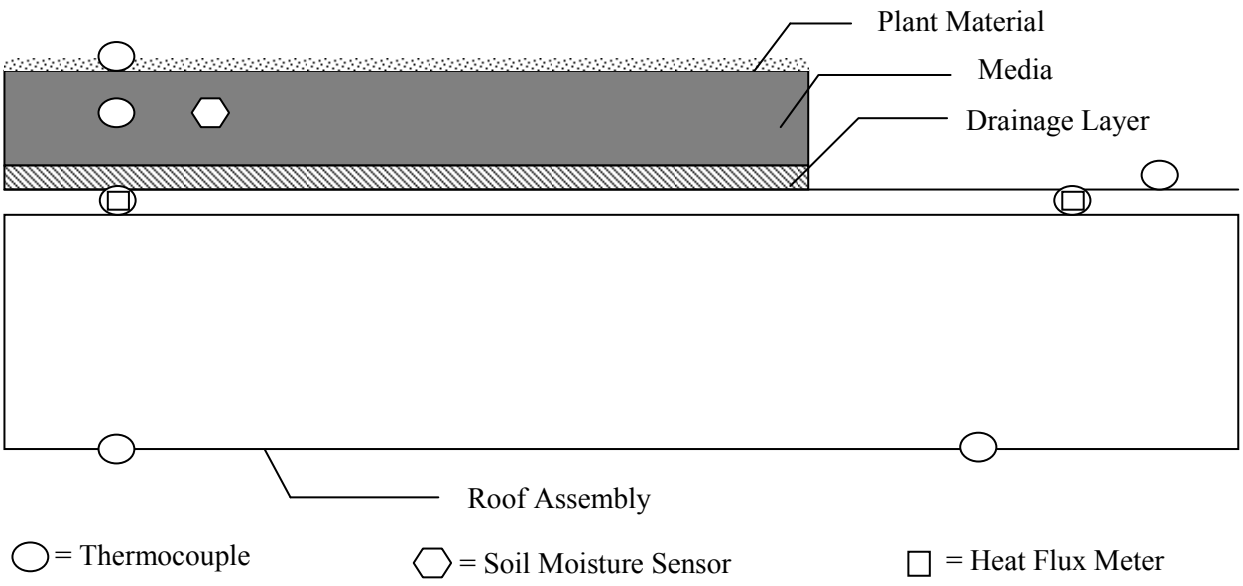

Figure **3.1**: Profile of Green Roof and Sensors.

3.1 Quality Control

Sensors in two different locations were used to measure the standard roof under membrane temperature, the green roof under membrane temperature, standard roof heat flux, and green roof heat flux. This was done for the sake of redundancy, to ensure that the data is accurate and backed up. As such, there are two sets of data for each variable. Before plotting these data, there needed to be some quality control; that is, it was important to verify that the results for each sensor location for a given variable correspond. Plots were made for one day at the beginning and one day at the end of each month. Based on the plots, it indeed seems that the

data for both of these measurements at each sensor location is fairly accurate and therefore, the data from the two sensors for a given variable may be averaged for simplicity before they are analyzed. Figures 3.2-3.5 were used for quality control.

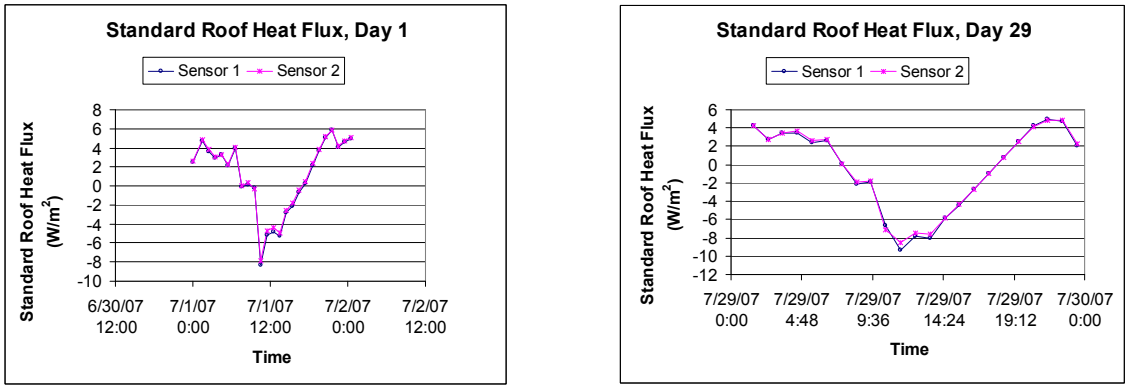

(a) (b)

Figure **3.2**: Standard Roof Heat Flux for (a) Day 1 and (b) Day 29.

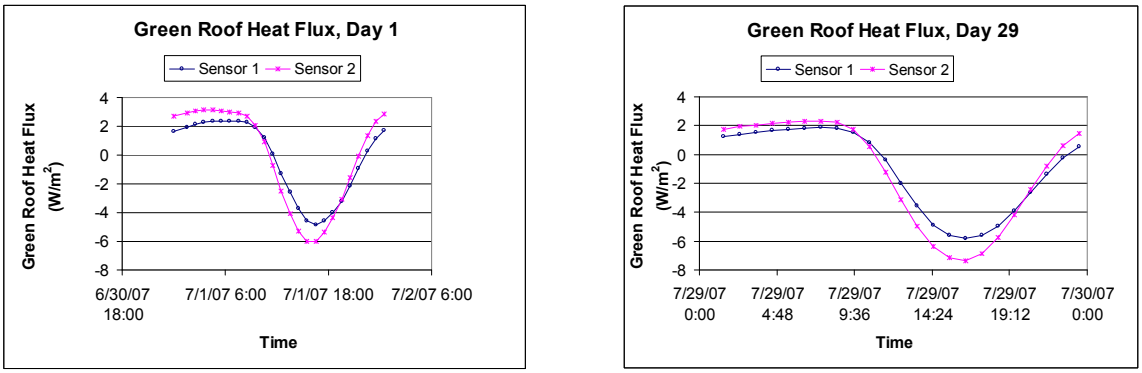

(a) (b)

Figure **3.3**: Green Roof Heat Flux for (a) Day 1 and (b) Day 29.

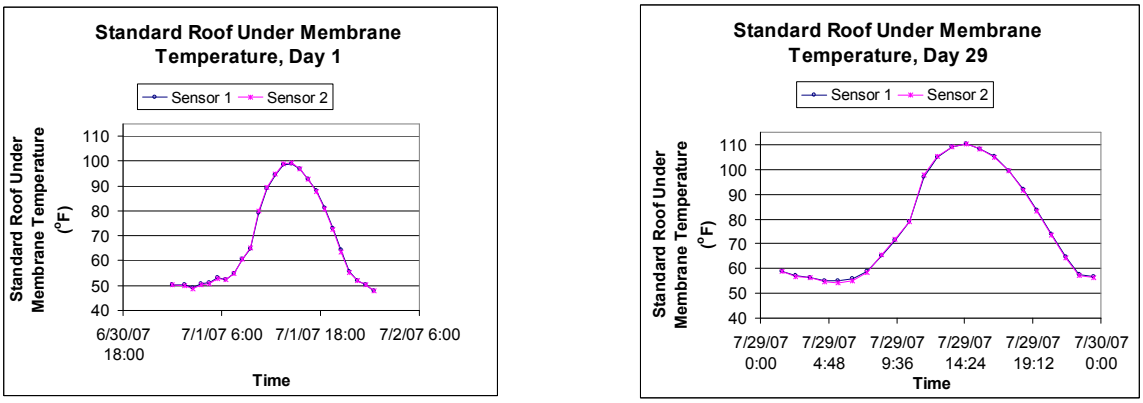

(a) (b)

Figure **3.4**: Standard Roof Under Membrane Temperature for (a) Day 1 and (b) Day 29.

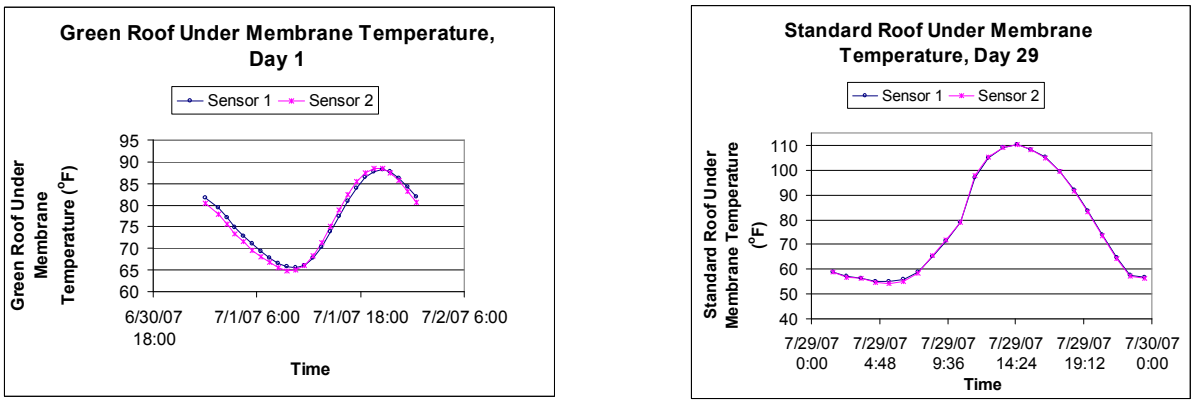

(a) (b)

Figure **3.5**: Green Roof Under Membrane Temperature for (a) Day 1 and (b) Day 29.

It should be noted that on the standard roof, there is really no variation with regard to the surface, whereas the green roof is a non homogenous material and thus one must take into account the Leaf Area Index (LAI) and other differences between the placements of the sensors, such as slight differences in soil thickness. The Leaf Area Index is defined as the leaf area divided by the soil surface (Tabares-Velasco, 2009); in essence, this means that the Leaf Area Index is the ratio of area that is covered by plants on a green roof. These differences in the curves for the measured variables on the green roof result in slight variations in the curves for the heat flux of the green roof at the two sensors, but not so much that their values cannot be averaged. For example, it was calculated that the maximum percentage difference for the green roof under membrane temperature is 2.17%, whereas the maximum percentage difference for the standard roof under membrane temperature is 1.45%.

3.2 Analysis

It is useful to compare certain variables with each other to find trends and peculiarities in the data. The following variables were investigated: Volumetric Water Content and precipitation, solar radiation and roof top wind speed, under membrane temperature for standard and green roofs, heat flux and solar radiation for standard and green roofs, and heat flux vs. Volumetric Water Content. For most of these variables, the data was first plotted week by week to see the overall trends occurring throughout the month. Subsequently, additional plots were made to focus more closely on specific features of the data sets.

3.2.1 Volumetric Water Content and Precipitation

By plotting Volumetric Water Content and Precipitation together, the relationship between the two—if there truly is one—can be seen more clearly. Volumetric Water Content is the amount of moisture that the soil will hold; it is defined as the volume of water divided by the total volume of the sample, or $VWC = V_{H20} / V_{total}$. Since this can be expressed as m^3/m^3, it is essentially dimensionless. Theoretically, the amount of rainfall affects the soil moisture. The question, then, is what kind of trends can be seen for a single month during summer? What is the average amount of precipitation and to what degree does that rainfall affect the soil moisture?

The data was collected and plotted in Figures 3.32-3.35 in the Appendix. However, upon a closer look at these plots, it was noted that although the peaks in precipitation varied from 0.0775 to 0.285 inches, the maximum value for Volumetric Water Content was measured consistently at 0.16. That is, no matter how much the rainfall, the soil moisture did not rise about this particular value. This lack of change of moisture content points to the likelihood of an error or limitations in instrumentation. The corrected maximum value of Volumetric Water Content

can be calculated utilizing two simple linear equations, as follows (Campbell Scientific, 2009a and Tabares-Velasco and Srebric, 2009b):

(1) VWC_data=0.0283 * period- 0.4677

(2) VWC_new=0.05 * period- 0.7479

Equation (1) is the manufacturer's calibration equation, while equation (2) is an equation specifically developed for this soil. The plots with the corrected values of Volumetric Water Content can be seen in Figures 3.7-3.10. Given the maximum value of about 0.16 for Volumetric Water Content from the data (VWC_data), the period can be found from equation (1). The period corresponding to this maximum value is 22.18 ms. Then, the corrected maximum value (VWC_new) can be determined from equation (2). This value is 0.36. This shows a percentage error between the manufacturer's calibration equation and that developed for the soil of 55.6%. This is not to say that the Volumetric Water Content must have always truly peaked at 0.36; however, this shows that the maximum capacity of water that the soil can hold is greater than is indicated in the data. In fact, the maximum amount of water that the soil can hold is 49.6%, as per the soil moisture report. This data was obtained from the green roof substrate test performed at the Agricultural Analytical Services Laboratory, The Pennsylvania State University. Past this value, the soil will begin draining. It should be noted that this runoff affects the drainage system of the building. However, since the soil and plants absorb much of the rainfall, there is less runoff for a green roof than there would be for a standard roof. This is a major benefit.

This concept of Volumetric Water Content and runoff can be explained further by looking into its definition and the equilibriums between the soil, air, and water in a particular

volume. The total volume is equal to combination of the volume of the soil, air, and water. This can be described with the following equation:

$$V_{total} = V_{soil} + V_{air} + V_{H20}$$

The volume of soil on the green roof remains constant. As the volume of water on the roof increases with rainfall, it replaces the volume where there was previously air, and so the volume of air decreases. Figure 3.6 depicts the situation in which there has been the maximum amount of rainfall before runoff. That is, the water has filled one half of this particular portion of the roof. If there were to be any more rainfall, the soil would no longer absorb the water and there would be runoff.

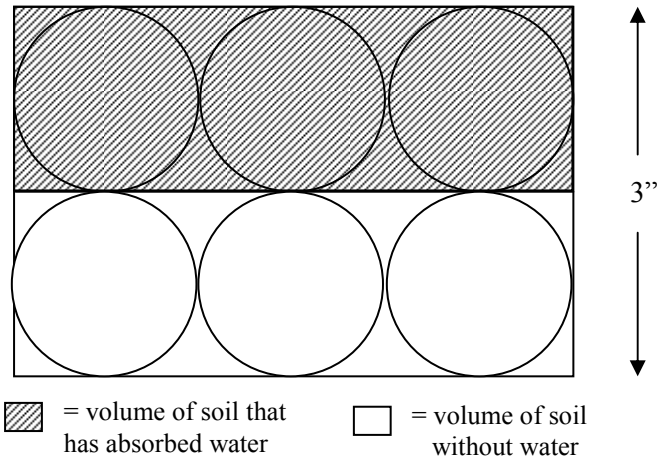

Figure **3.6**: Diagram of Section of Green Roof and Absorbed Rainfall.

This concept may be utilized as follows. The total precipitation in a specific event should give an indication of how much the Volumetric Water Content should increase over that same period. From 11:30pm on July 3rd to 3:30pm on July 4th, the total rainfall was 0.54 inches, while the increase in the Volumetric Water was 0.17%. Rearranging the equation for Volumetric Water Content and substituting in the appropriate values,

$$V_{total} = VWC * V_{H20} = (3”)(.17) = 0.51”$$

Since 0.51 inches is much less than half of 3 inches, this indicates that there was likely no runoff on the green roof during this specific event. Other events can be analyzed in the same manner.

Figures 3.7-3.10 show the plots with the corrected values of Volumetric Water Content.

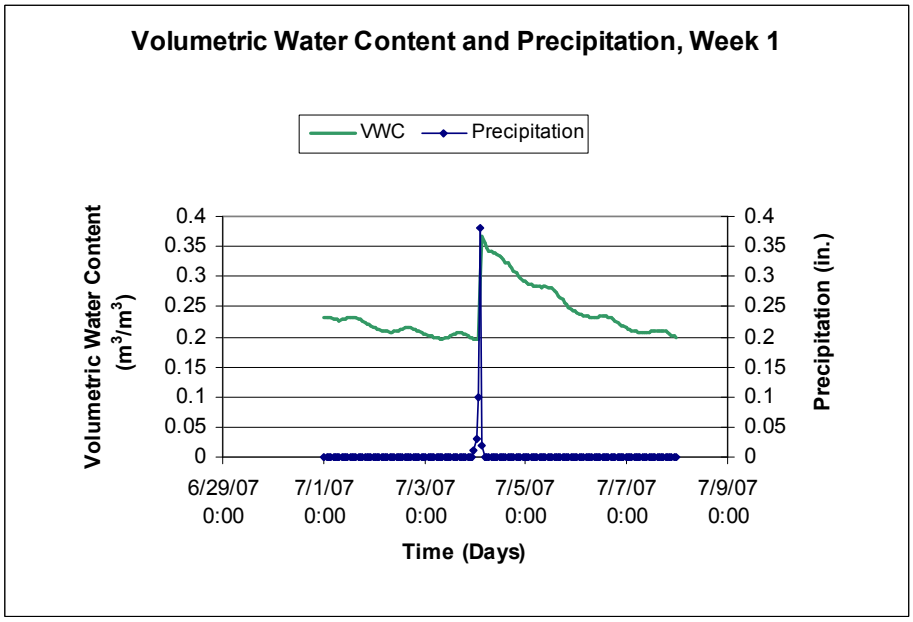

Figure **3.7**: Volumetric Water Content and Precipitation, Week 1.

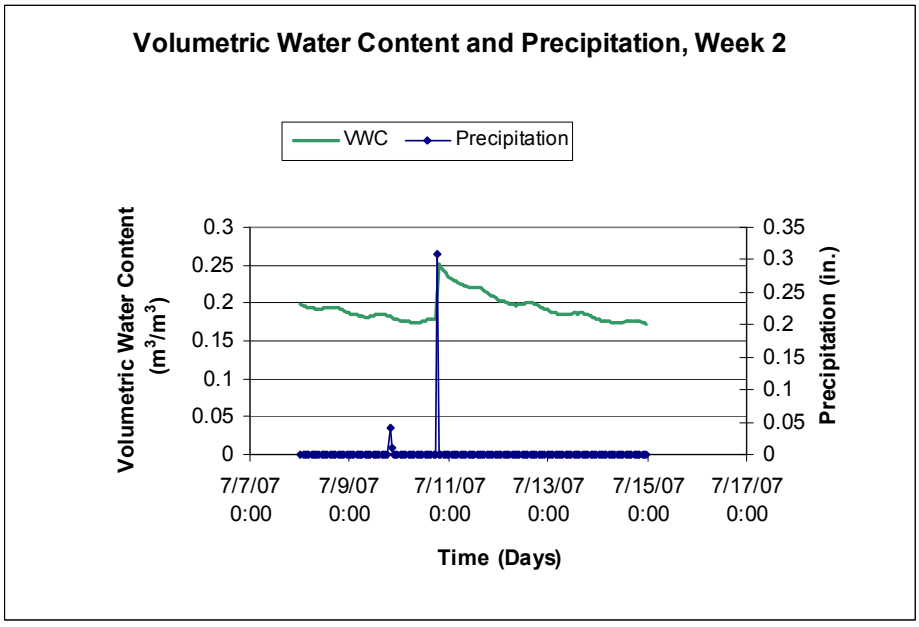

Figure **3.8**: Volumetric Water Content and Precipitation, Week 2.

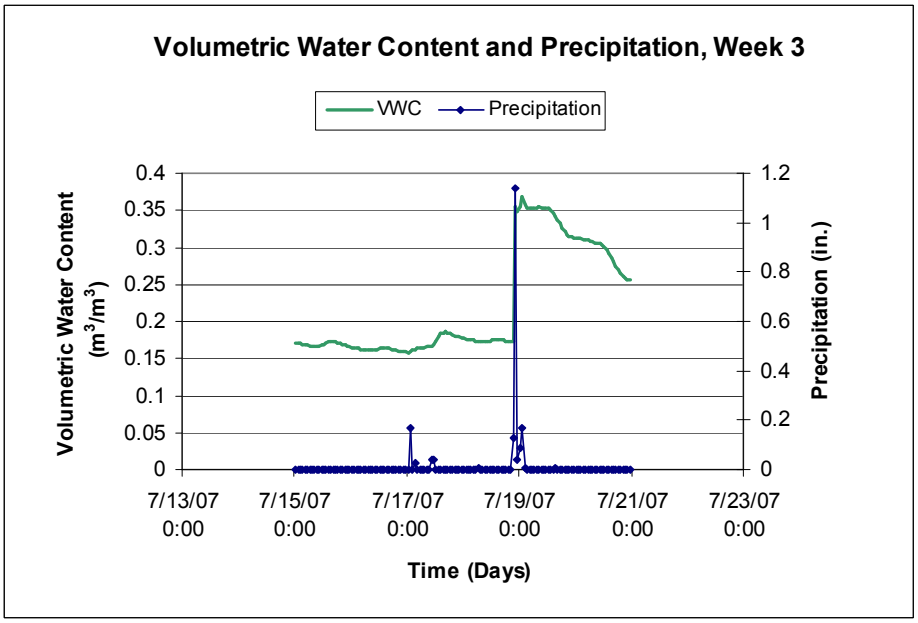

Figure **3.9**: Volumetric Water Content and Precipitation, Week 3.

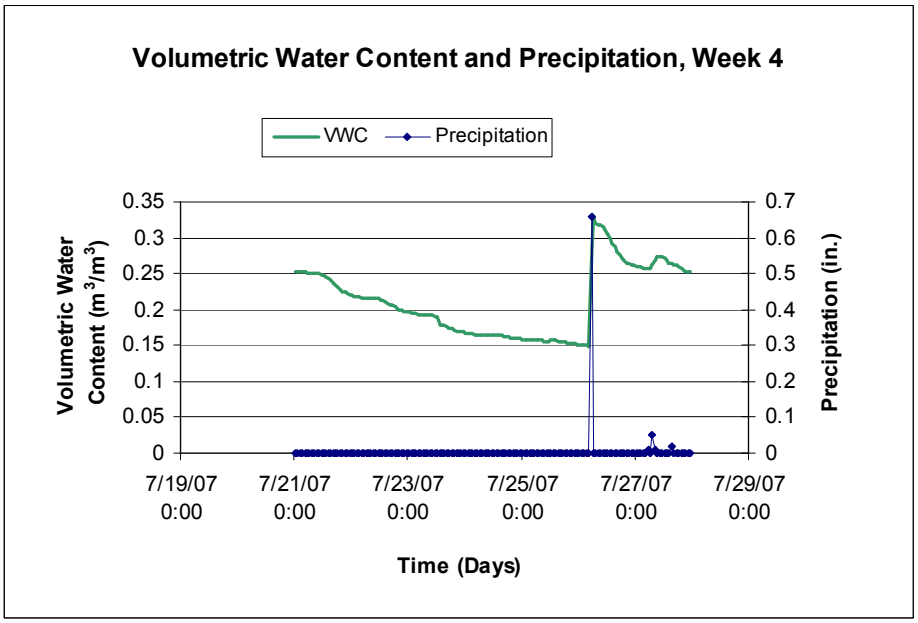

Figure **3.10**: Volumetric Water Content and Precipitation, Week 4.

After viewing the weekly plots of Volumetric Water Content and Precipitation, it is clear that for much of the month, there was no rainfall. In fact, the average rainfall for the month was 0.0049 inches. However, the precipitation does peak at 1.14 inches, and the total rainfall for the

month was 3.53 inches. It should be noted that the peak precipitation occurred on July 18, 2007. The data for this week should be looked at more closely, as shown in Figure 3.11. This shows that, as would be expected, when the precipitation peaks, the soil moisture is at its peak as well. After the precipitation peak, the soil moisture decreases slowly until the next precipitation peak about a week later, at which point, the cycle begins again. This plot shows the entire cycle quite clearly.

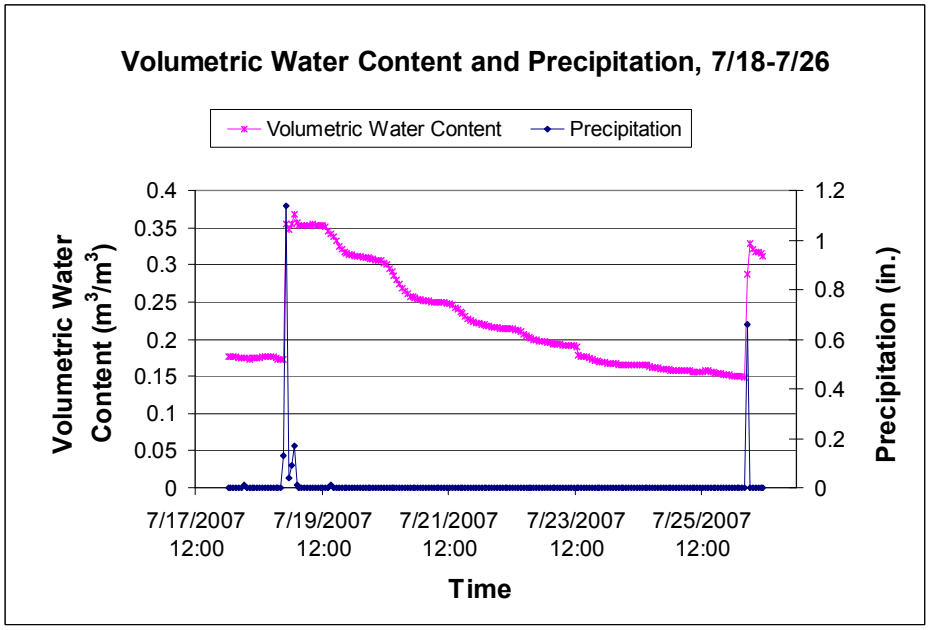

Figure **3.11**: Volumetric Water Content and Precipitation, 7/18-7/26.

3.2.2 Solar Radiation and Roof Top Wind Speed

By plotting solar radiation and roof top wind speed, information can be uncovered regarding climate conditions during the month of July. See Figures 3.12-3.15.

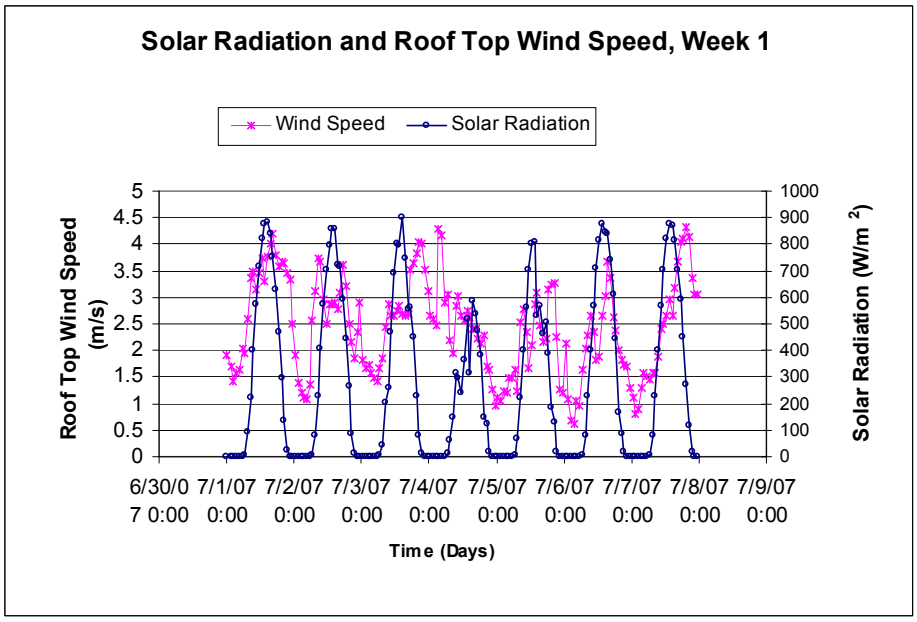

Figure **3.12**: Solar Radiation and Roof Top Wind Speed, Week 1.

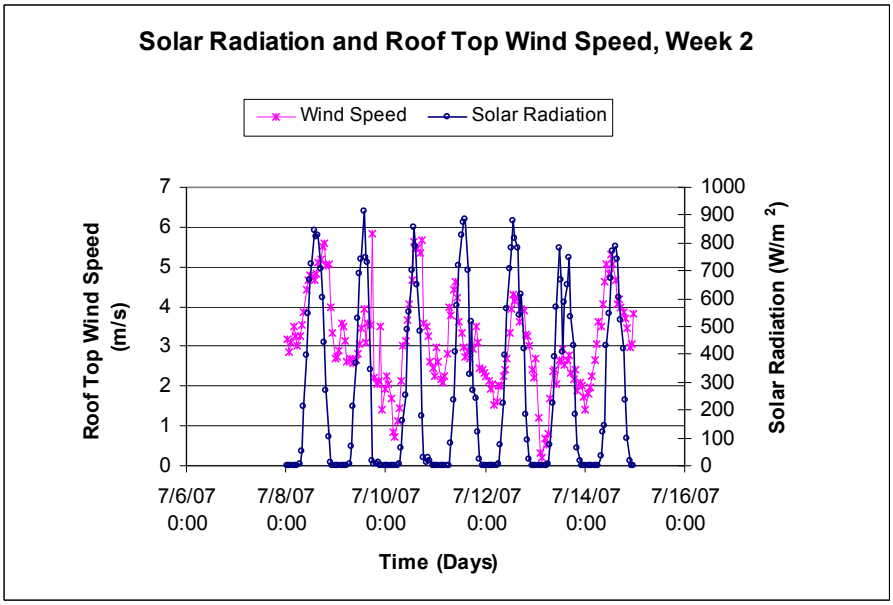

Figure **3.13**: Solar Radiation and Roof Top Wind Speed, Week 2.

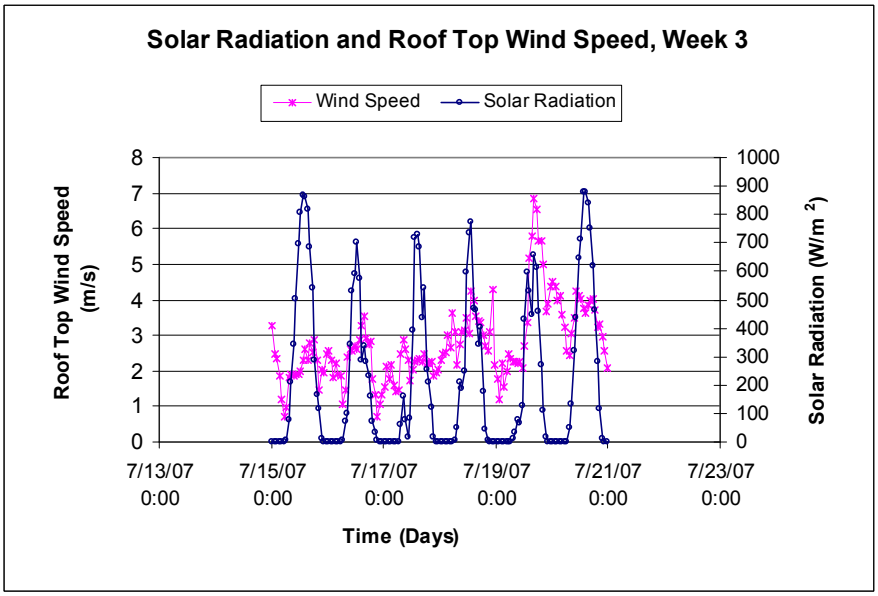

Figure **3.14**: Solar Radiation and Roof Top Wind Speed, Week 3.

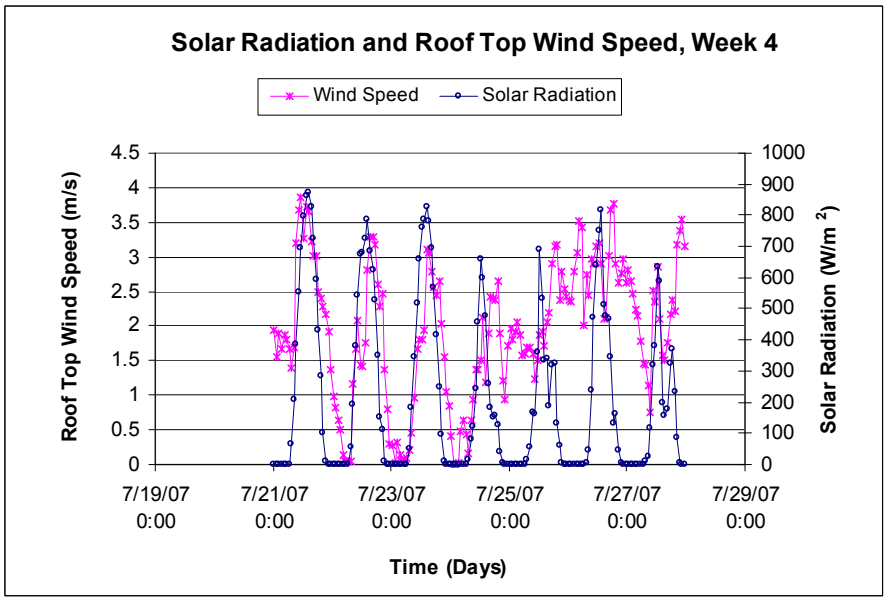

Figure **3.15**: Solar Radiation and Roof Top Wind Speed, Week 4.

From Figures 3.12-3.15, one can see that most days had high radiation values and the peak incoming radiation was about 913 W/m^2. The minimum value was 0.034 W/m^2. It should be noted that the high values of solar radiation indicate that it is likely that there was a good amount of sunlight reaching the roofs; that is, there were, for the most part, clear skies (Duffie

and Beckman, 1991). The maximum roof top wind speed was 15.3 mph, or 6.84 m/s, and the minimum value was 0.0875 mph, or 0.0039 m/s. Typically, the roof top wind speed peaked during early evening—anytime between 4:30pm and 7:30pm—and was at a minimum at around 1:30 to 2:30am. There are, of course, some exceptions, such as the continuous high values of wind speed from 7:30pm on 7/25/2007 to 6:30pm on 7/26/2007; during this time, the value did drop, but not very much. The week of 7/18-7/26 is again plotted in Figure 3.16.

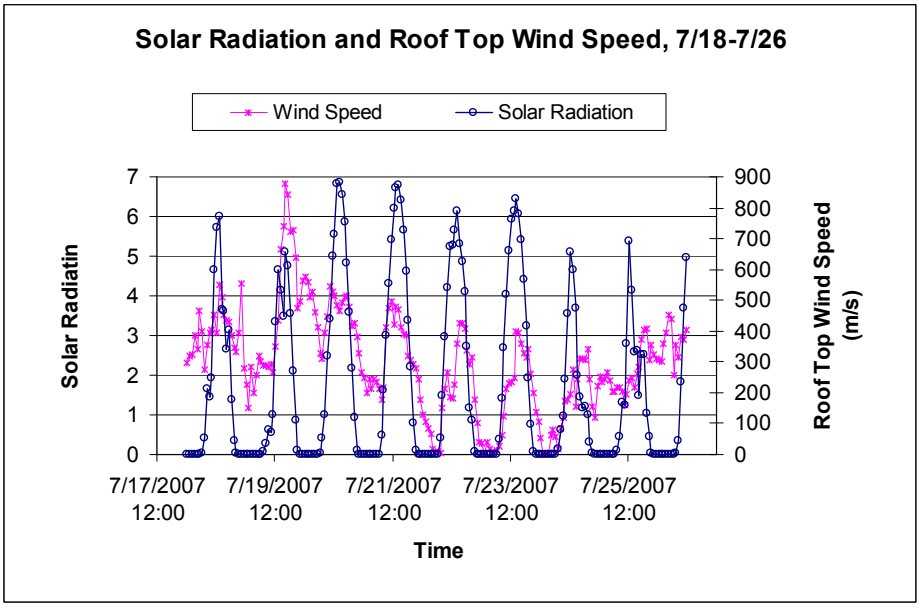

Figure **3.16**: Solar Radiation and Roof Top Wind Speed, 7/18-7/26.

3.2.3 Under Membrane Temperature for Standard and Green Roofs

The under membrane temperature can be compared for the standard and green roofs. Since the materials on these roofs are very different, it can be assumed that the temperature will fluctuate differently. See Figures 3.17-3.20.

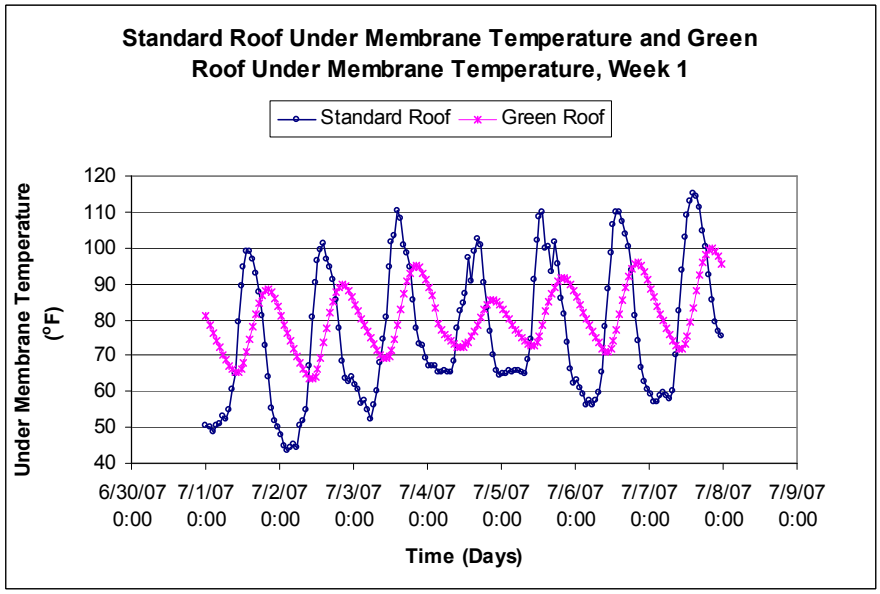

Figure **3.17**: Under Membrane Temperature, Week 1.

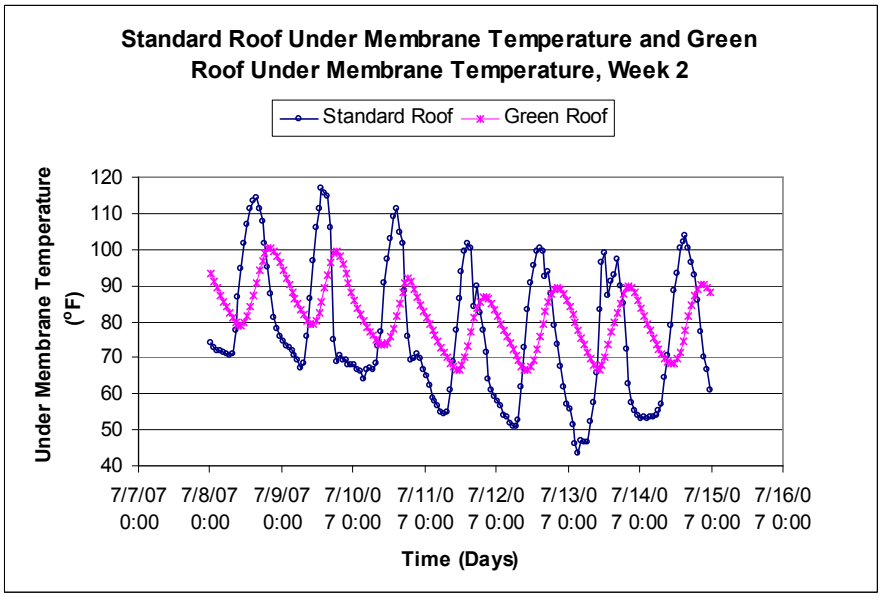

Figure **3.18**: Under Membrane Temperature, Week 2.

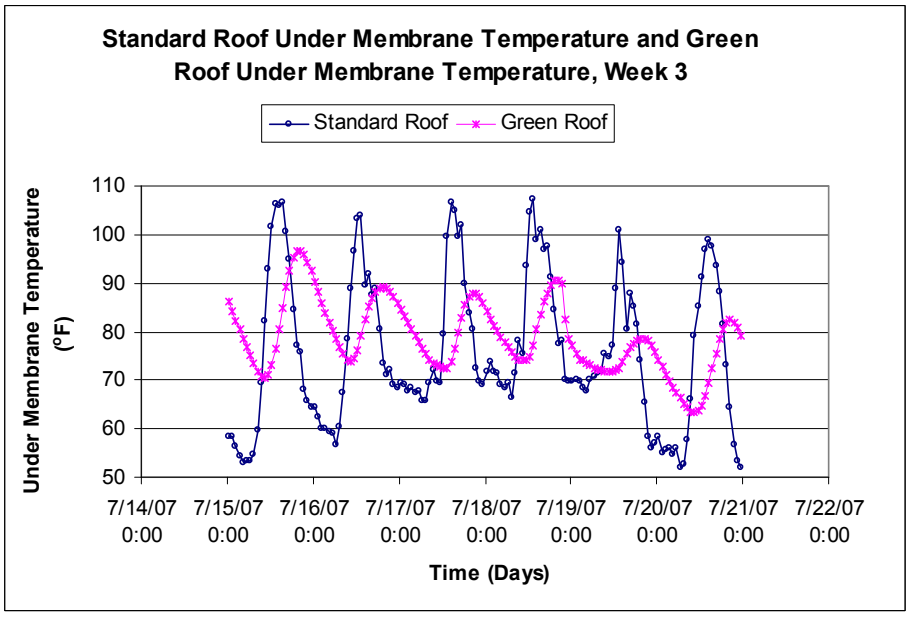

Figure **3.19**: Under Membrane Temperature, Week 3.

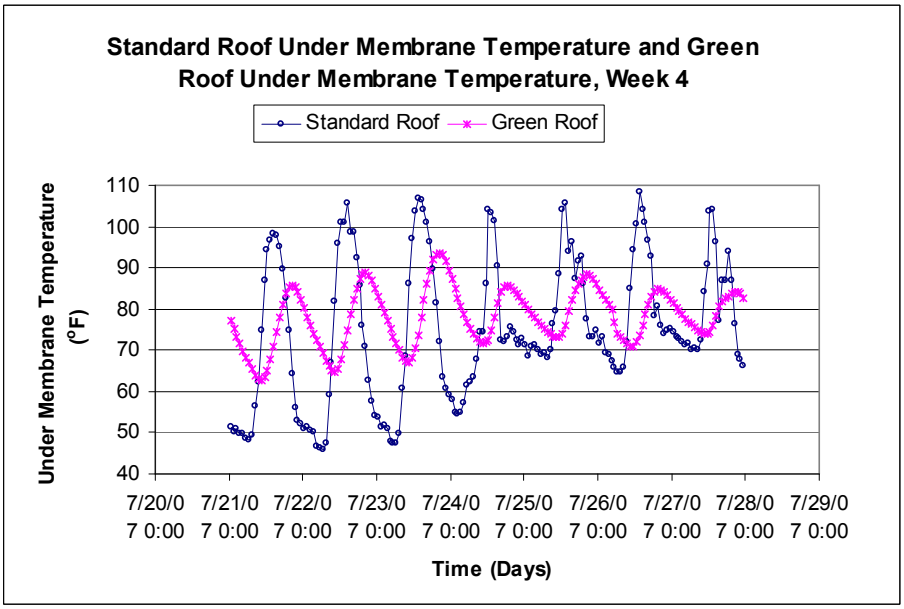

Figure **3.20**: Under Membrane Temperature, Week 4.

From Figures 3.17-3.20, one can see that the maximum under membrane temperature was 116.8°F for the standard roof and about 100°F for the green roof. Comparing the values during the day and at night, certain trends can be seen; the standard roof under membrane temperature

consistently peaked from 1:30pm to 4:30pm, while the green roof under membrane temperature consistently peaked from 7:30pm to 10:30pm. Similarly, the standard roof under membrane temperature is at a minimum in the early morning hours from 2:30am-7:30am, while the green roof under membrane temperature is at a minimum later in the morning at around 10:30am-12:30pm. In essence, the temperature oscillations are offset by a few hours. Moreover, the variation from day to night of the under membrane temperature is about 50°F for the standard roof, whereas the variation for the green roof is only 20°F. Less under membrane temperature variation translates to less stress on the water proof membrane due to thermal expansion and contraction. This decrease in variation may be considered a benefit of the green roof over the standard roof.

3.2.4 Heat Flux for Standard and Green Roofs

Finally, the heat flux was analyzed. This analysis is perhaps the most integral, as it will indicate the performance of the green roof as compared to the standard roof. By determining if the green roof reduces heat flux, conclusions can be made as to whether or not green roof technology is effective in reaching its goals with regard to heat and mass transfer. See Figures 3.21-3.25 for heat flux curves for the standard and green roofs.

It should be noted that for this data, the original convention stated that positive heat flux values represented outgoing heat flux, while negative heat flux values represented incoming heat flux. However, for the sake of simplicity and ease of understanding, the opposite convention was employed in this thesis. As such, the heat flux data was altered simply by negating the data.

Then, the convention is that positive values represent incoming heat flux while negative values represent outgoing values.

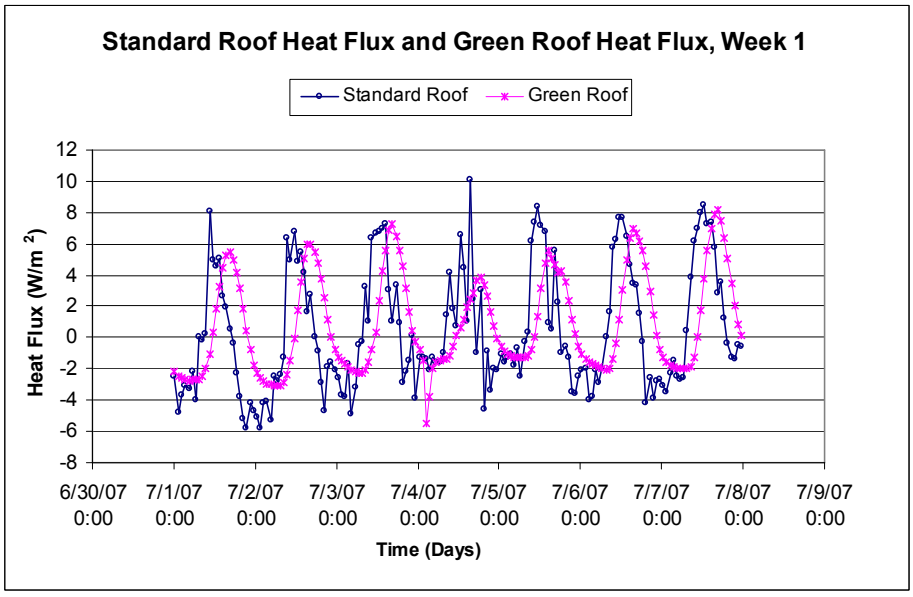

Figure **3.21**: Heat Flux for Standard and Green Roofs, Week 1.

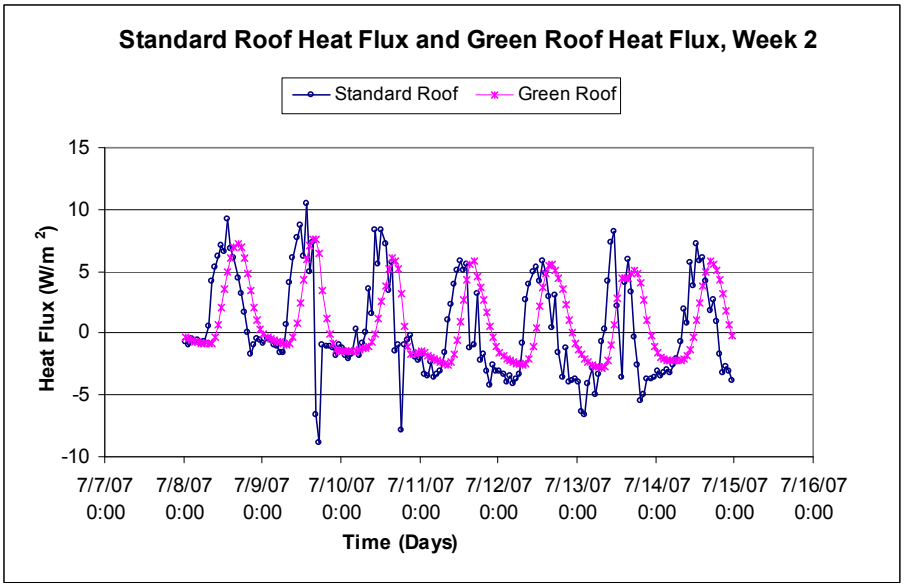

Figure **3.22**: Heat Flux for Standard and Green Roofs, Week 2.

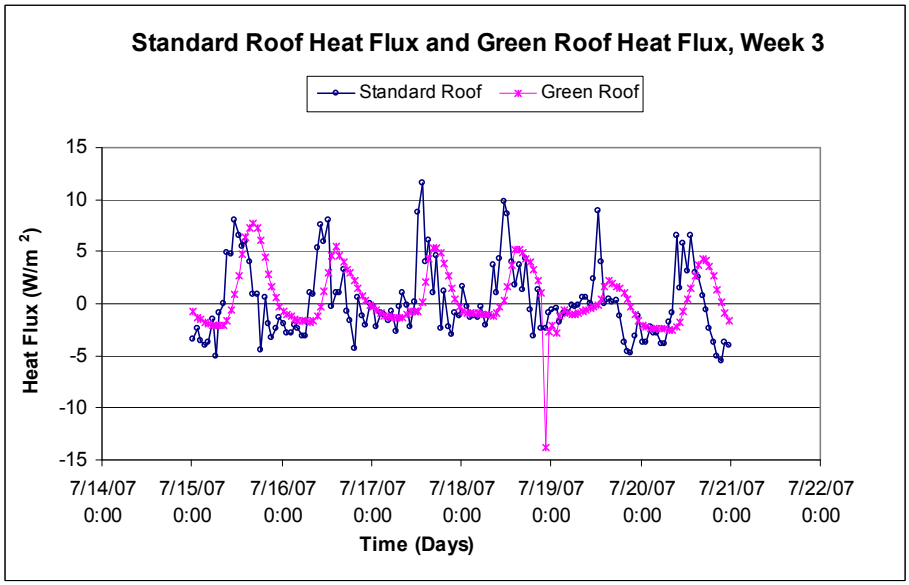

Figure **3.23**: Heat Flux for Standard and Green Roofs, Week 3.

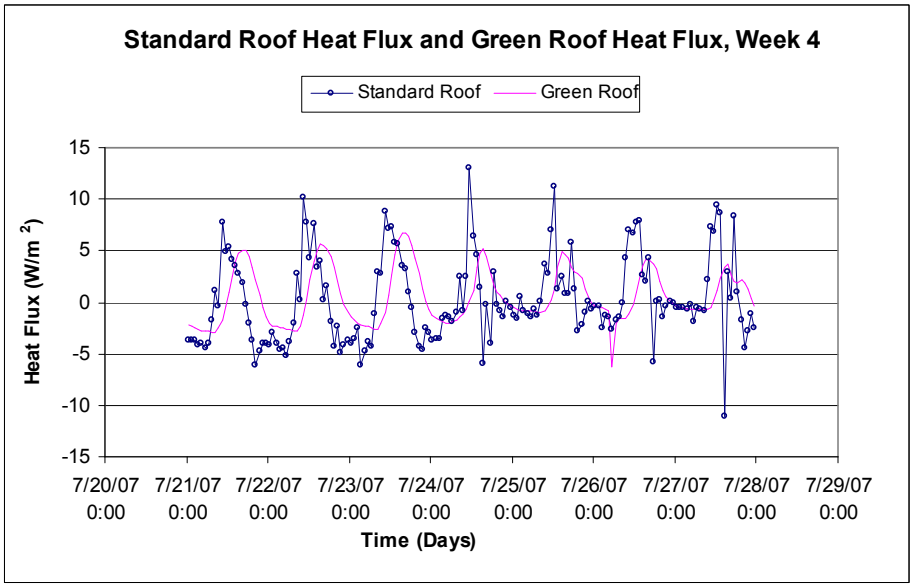

Figure **3.24**: Heat Flux for Standard and Green Roofs, Week 4.

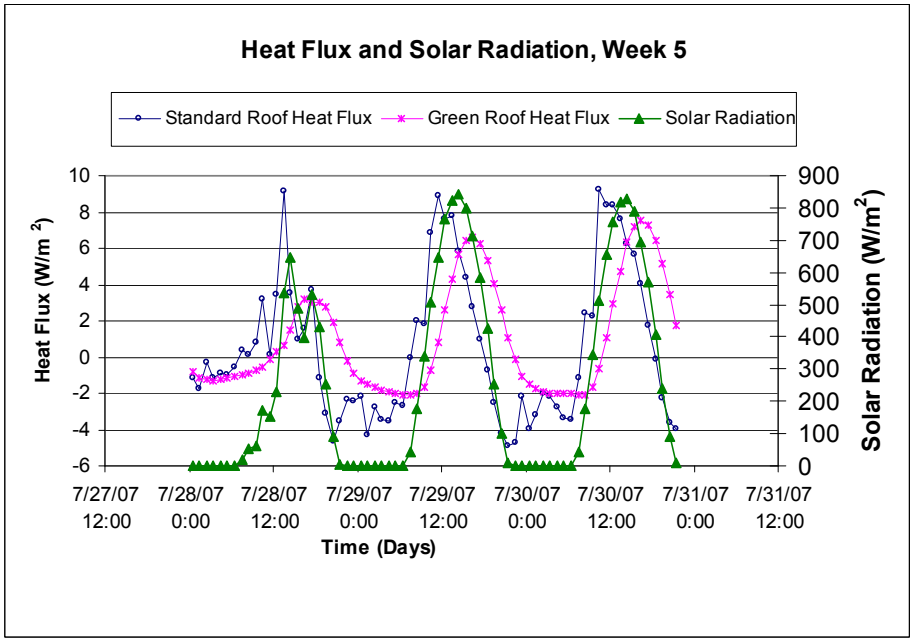

Figure **3.25**: Heat Flux and Solar Radiation, Week 5.

First of all, from Figure 3.25, it seems that the solar radiation peaks around the same time that the heat flux for both the standard and green roofs peak. Then, from Figures 3.21-3.24, it is clear that the oscillations for heat flux for both the green roof and the standard roof are fairly similar; however, there are certain characteristics that stand out. The incoming heat flux peaks at about 13 W/m^2 and 8 W/m^2 for the standard roof and green roof, respectively. However, in general, the incoming maximum values tend to be much lower; for the standard roof, the oscillations seem to smooth out around 7 to 11 W/m^2 and around 5 to 8 W/m^2 for the green roof. The incoming maximum values for the green roof occur several hours after that of the incoming maximum values for the standard roof. These incoming maximum values occur during the day. The maximum outgoing values for the standard and green roof—occurring at night—are around -4 to -9 W/m^2 and -0.7 to -3 W/m^2, respectively. The peaks for these values are slightly offset as well; the outgoing maximum values for the green roof occur a couple hours after that of the

outgoing maximum values for the standard roof. It is important to note that the heat flux during the day is incoming since heat is being transferred from the outside environment to the system, the building, while the heat flux during the night is outgoing since heat is being transferred from the building to the outside environment. Furthermore, these numbers show that the magnitude of the heat flux for the green roof is not quite as large as that of the standard roof, and it is also a bit of a smoother curve. This is likely due to the fact that the soil on the green roof, along with processes such as evapotranspiration and shading, damps and decreases the oscillations. Other studies have found similar results (Liu et al., 2004). These differences in values between the standard and green roofs can be analyzed further with statistical analysis.

The daily incoming heat flux was calculated for both the standard roof and the green roof. This calculation was based on the averaged values from the sensors placed on each roof. There are several methods to do this. The most direct way is to simply add the hourly heat flux values for a 24-hour period, which gives a rough estimation of total heat flux. Table 3.1 shows these values for the month of July, along with the daily solar radiation and the net radiation for the standard and green roofs, which were calculated in a similar fashion. Figure 3.26, based on the table, can be used to compare the trends of the heat flux for the standard roof and the green roof.

Table **3.1**: Total Heat Flux, Daily Solar Radiation, and Net Radiation for the month of July.

Day	Total Heat Flux (W·hr/m2·day)		Daily Solar Radiation (W·hr/m2·day)	Net Standard Roof Radiation (W·hr/m2·day)	Net Green Roof Radiation (W·hr/m2·day)
	Standard roof	Green roof			
1	-21.67	6.57	322.67	43.04	178.89
2	-10.28	9.71	306.12	38.22	170.38
3	16.04	28.81	283.76	34.06	158.13
4	10.57	4.30	189.24	18.42	114.26
5	23.10	28.93	265.36	33.75	161.37
6	13.49	32.45	310.19	42.37	176.61
7	39.91	41.98	313.40	43.63	188.72
8	52.92	50.12	301.54	47.66	197.70
9	26.63	37.26	224.55	17.84	116.88
10	18.49	15.14	218.90	33.94	147.74
11	-9.38	7.54	283.29	35.03	159.71
12	-5.26	14.38	296.46	40.70	169.46
13	-25.28	13.89	263.60	31.91	129.57
14	5.49	16.45	256.62	36.12	152.95
15	4.46	34.41	291.67	34.15	145.26
16	6.49	19.52	180.38	19.26	88.54
17	16.42	17.53	187.97	5.52	96.56
18	28.23	9.24	196.57	27.69	122.81
19	-6.22	-4.99	185.53	27.25	125.20
20	-21.23	-3.88	297.82	40.70	184.19
21	-23.24	2.17	309.20	40.53	174.87
22	-10.35	11.01	270.60	31.89	149.63
23	0.26	24.35	289.53	38.27	157.93
24	1.72	7.61	149.04	12.13	69.14
25	22.90	23.44	153.45	18.43	82.24
26	23.75	8.09	213.08	33.03	148.20
27	16.91	15.93	151.21	6.57	83.24
28	2.97	7.82	169.43	29.28	107.98
29	8.21	25.63	293.28	38.75	166.68
30	24.09	34.14	288.70	41.08	161.37
sums:	230.14	539.55	7463.15	941.25	4286.21

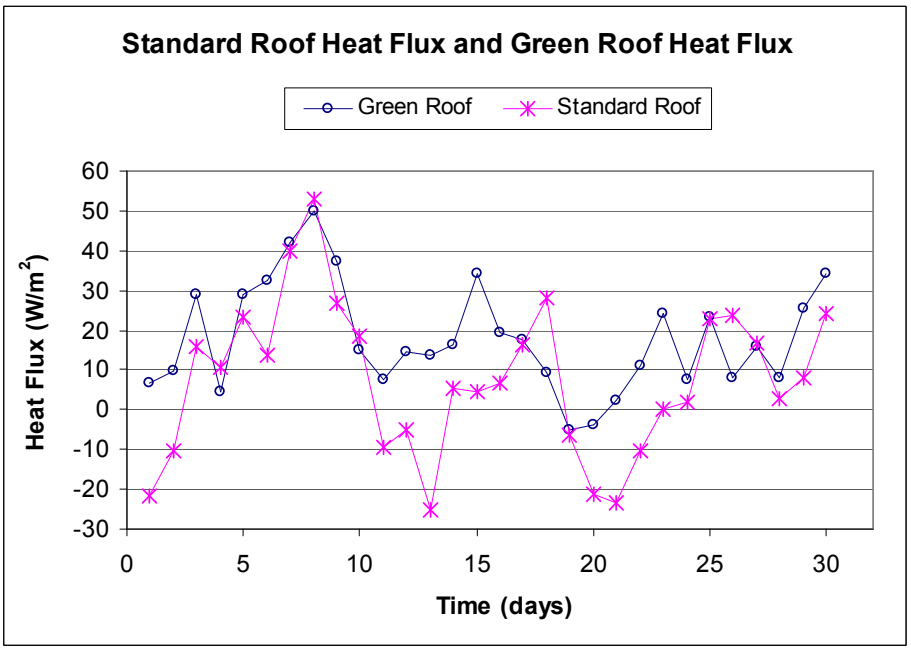

Figure **3.26**: Total Heat Flux for the month of July.

Once the daily incoming heat flux was calculated, the data could be statistically analyzed to verify that the heat flux for the standard and green roofs differ. This analysis is significant, as this would be a good indication—based on this particular experiment—of whether or not green roofs are effective in lowering the heat flux to a building.

From Table 3.1, it is clear that the total monthly heat flux for the green roof is higher than that of the standard roof, which is not favorable. The alternative hypothesis can be stated as H_a: $\Pi_{GR} > \Pi_{SR}$, where Π_{GR} represents the heat flux for the green roof and Π_{SR} represents the heat flux for the standard roof. Then, the null hypothesis is stated as H_o: $\Pi_{GR} \leq \Pi_{SR}$. Using Excel's Data Analysis tool with "t-Test: Two-Sample Assuming Equal Variances," and assuming that the level of significance, or probability of a Type I error (rejection of H_o), α, is 0.05, the t-statistic and p-value could be found.

Table **3.2**: Two Sample t-test for Heat Flux of Green and Standard Roofs.

t-Test: Two-Sample Assuming Equal Variances

	Variable 1	*Variable 2*
Mean	7.671204	17.98515
Variance	359.4311	183.3868
Observations	30	30
Pooled Variance	271.4089	
Hypothesized Mean Difference	0	
df	58	
t Stat	-2.4247	
P(T<=t) one-tail	0.009228	
t Critical one-tail	1.671553	
P(T<=t) two-tail	0.018457	
t Critical two-tail	2.001717	

As seen in Table 3.2, the t-statistic is -2.42 and the p-value is 0.009228. The p-value is less than α, and thus we may reject the null hypothesis. This means that we are 95% confident that the heat flux to a building with a green roof is higher than that of a building with a standard roof. To illustrate this point, one may look directly at the numbers. The sums of the daily incoming heat flux for the green and standard roofs are 539.55 and 230.14 W·hr/m2·month, respectively. Indeed, the incoming heat flux for the green roof is higher. Additionally, the difference between the sums of the heat flux for the standard and green roofs is the savings. In this case, the savings for the standard roof is 309 W·hr/m^2·month, or 57%. It should be noted that with these findings, it must be taken into account that the "standard" roof is a white reflective roof, which means that it reflects incoming radiation. Thus, these results were somewhat expected. Unfortunately, there is no standard black roof to use for comparison.

Although these numbers show that the standard roof performs better than the green roof with regard to the total monthly heat flux, the green roof still decreases the load of the heat flux, meaning that it may not be necessary to run the air conditioning as much, and this results in peak

energy savings. This is a major benefit. Moreover, these numbers show that the white reflective roof performs better than the green roof; however, more data would need to be analyzed to determine how a green roof performs as compared to a standard black roof.

A second method to calculate the total daily heat flux is to calculate the area under the curve. This method may help verify the findings. Once one day of data has been plotted, a trendline can be added to both the green roof heat flux curve and the standard heat flux curve, and the polynomial equation can be displayed. In this case, a sixth-order polynomial obtains the best R^2 value, and consequently, the best correlation. The daily heat flux can be found by integrating these equations. Figure 3.27 shows the first day of data, with the polynomial equations and correlation coefficient, R^2, values displayed beneath the graph.

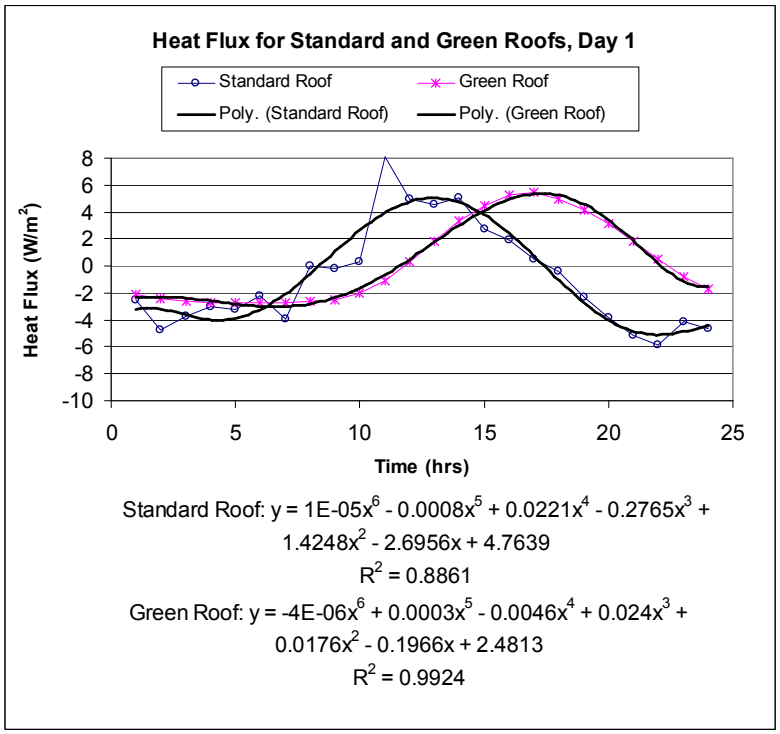

Figure **3.27**: Heat Flux for Standard and Green Roofs, Day 1.

The equations for the trendlines can also be found using Engineering Equation Solver (EES). The equations from EES are as follows:

Standard roof:
Q_R=4.7639334 - 2.69558337*time + 1.42478057*time^2 - 0.276539395*time^3 + 0.0220909995*time^4 - 0.00077144383*time^5 + 0.00000983794107*time^6

Green roof:
Q_GR=4.52022643 - 2.62544318*time + 0.874668785*time^2 - 0.105613245*time^3 + 0.00491928631*time^4 - 0.0000773117633*time^5

It was found that the number of significant figures that Excel outputs for the trendline equations is not sufficient, and thus, the calculated heat flux was found to be very high. Employing EES, much more accurate values can be found. The daily heat flux calculated from these equations is -17.8 $W \cdot hr/m^2 \cdot day$ for the standard roof and 8.96 $W \cdot hr/m^2 \cdot day$ for the green roof. These values are fairly close to those found using the previous method, and may be compared to the values in Table 3.1 for day 1. It should be noted that, as found in Excel, the R^2 values are 0.8861 and 0.9924 for the standard and green roofs, respectively. The differences in these values can be explained simply by looking at the graphs and understanding the effect that the green roof has with regard to decreasing oscillations of the heat flux. Since the heat flux for the green roof yields a smoother curve, the corresponding trendline follows the curve fairly well. On the other hand, the curve for the standard roof heat flux is less smooth and the trendline cannot account for these sharp spikes. Thus, the correlation value for the green roof is much higher than that of the standard roof.

Finally, the convective heat transfer coefficient can be calculated for the standard roof using the following equation (Tabares-Velasco and Srebric, 2009a):

$$R_n = ET + Q_{sensible} + Q_{conduction} + S_{thermal} + M$$

where

R_n = net radiation, equal to solar gain minus infrared heat losses, $Btu/hr \cdot ft^2$ (W/m^2),

ET = evapotranspiration, or latent heat flux, $Btu/hr \cdot ft^2$ (W/m^2),

$Q_{sensible}$ = convective or sensible heat flux, Btu/hr·ft^2 (W/m^2),

$Q_{conduction}$ = heat flux through roof, Btu/hr·ft^2 (W/m^2),

$S_{thermal}$ = thermal storage for substrate, plants, Btu/hr·ft^2 (W/m^2), and

M = metabolic storage (photosynthesis and respiration), Btu/hr·ft^2 (W/m^2).

Since there are no plants, evapotranspiration, ET, and metabolic storage, M, can be neglected. Furthermore, assuming quasi-steady state conditions, the thermal storage for substrate, $S_{thermal}$, can be neglected. Thus, the equation becomes:

$$R_n = Q_{sensible} + Q_{conduction}$$

The heat flux through the roof, $Q_{conduction}$, and the net radiation, R_n, are both known, and therefore, the equation may be solved for the convective or sensible heat flux. Then, the convective heat flux can be written in equation form as follows:

$$Q_{sensible} = h\Delta T$$

where

h = the convective heat transfer coefficient and

ΔT = the difference between the surface temperature of the roof and the air temperature.

The temperature change is the difference between the surface temperature of the roof and the air temperature. Using the values for $Q_{sensible}$, the convective heat transfer coefficient can be calculated. Figures 3.28-3.29 show the convective heat transfer coefficient plotted with the roof top wind speed and the difference in temperature for the first week of data.

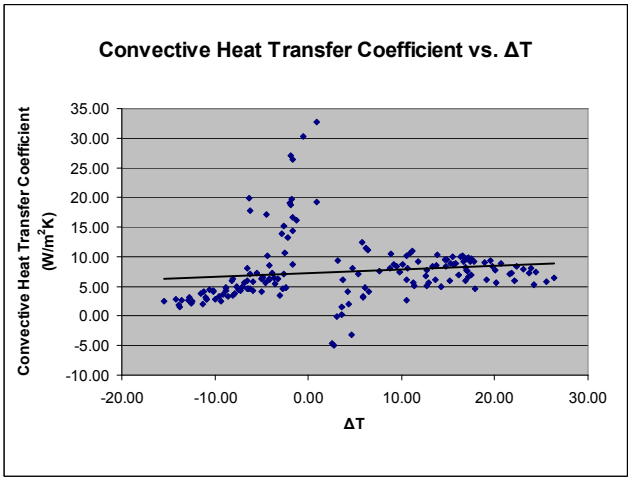

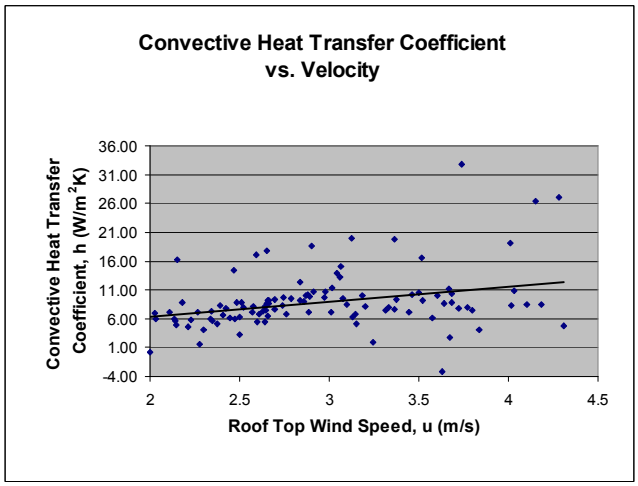

Figure **3.28**:Convective Heat Transfer Coefficient vs. ΔT. Figure **3.29**:Convective Heat Transfer Coefficient vs.u.

From figures 3.28-3.29, it may be observed that these data do not appear to have strong trends. To support this notion, the correlation coefficients, or R^2 values, may be considered. The R^2 value for the convective heat transfer coefficient versus the temperature difference is 0.0175, while the, R^2 value for the convective heat transfer coefficient versus the roof top wind speed is 0.1934. Both of these values are much lower than 1, which would indicate that neither the temperature difference nor the roof top wind speed has a strong correlation to the convective heat transfer coefficient for this particular data set.

The convective heat transfer coefficient can be analyzed further. It is likely that the convection on this roof was forced convection, rather than free, due to high wind speed conditions. Thus, the convection heat transfer coefficient can be solved using a second method, as it is a function of the Reynolds number. The equation for this relationship is:

(3) $h = 0.037*Re_L^{0.8}*Pr^{1/3}$

where

Re = Reynolds number

Pr = Prandtl number

The Prandtl number is dependent on medium and is found to be 0.707 for an average air temperature of 300 K (Incropera et al., 2008). The Reynolds number is defined as:

(4) $Re_L = uL/\nu$

where

u = velocity, or roof top wind speed

L = characteristic length

ν = kinematic viscosity

The characteristic length can be calculated. Given that the total area of the roof is 150,000 ft^2 and assuming that the roof is square, the characteristic length is 118 meters. The kinematic viscosity is found to be 15.89 x 10^6 m^2/s for an average air temperature of 300 K (Incropera et al., 2008).

Solving for the Reynolds number using equation (4) and substituting these values into the equation (3), the convective heat transfer coefficient may be found. A plot of convective heat transfer coefficient versus the Reynolds number for the month of July is shown in Figure 3.30.

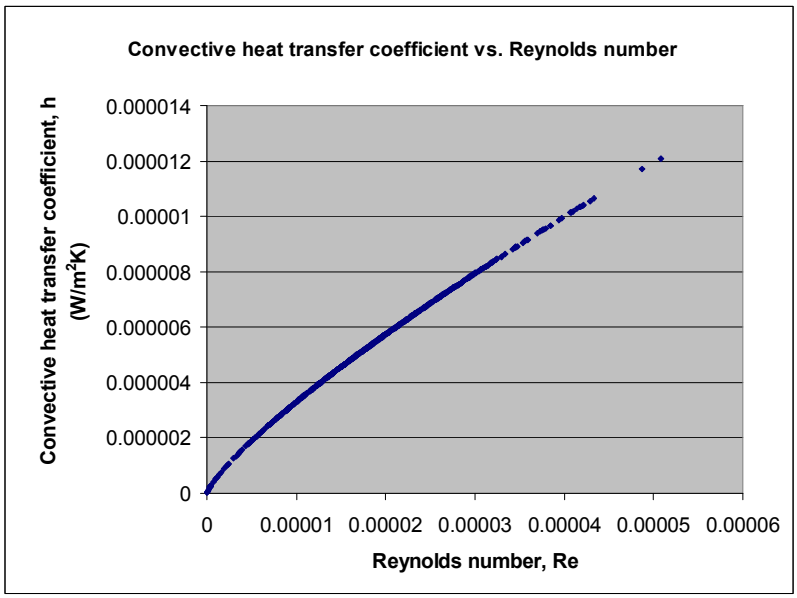

Figure **3.30**: Convective heat transfer coefficient vs. Reynolds number

Figure 3.30 shows that the Reynolds number and the convective heat transfer coefficient have a strong correlation, which is expected, as the convective heat transfer coefficient is a function of the Reynolds number. In fact, the correlation coefficient for these data is 0.9932. Furthermore, the Reynolds number and the convective heat transfer coefficient have a linear relationship.

4.2.5 Volumetric Water Content and Heat Flux

Finally, the heat flux may be plotted against the Volumetric Water Content to examine if there are any trends or correlations between the two variables. Figure 3.31 shows this plot, complete with trendlines for the data for the standard and green roofs.

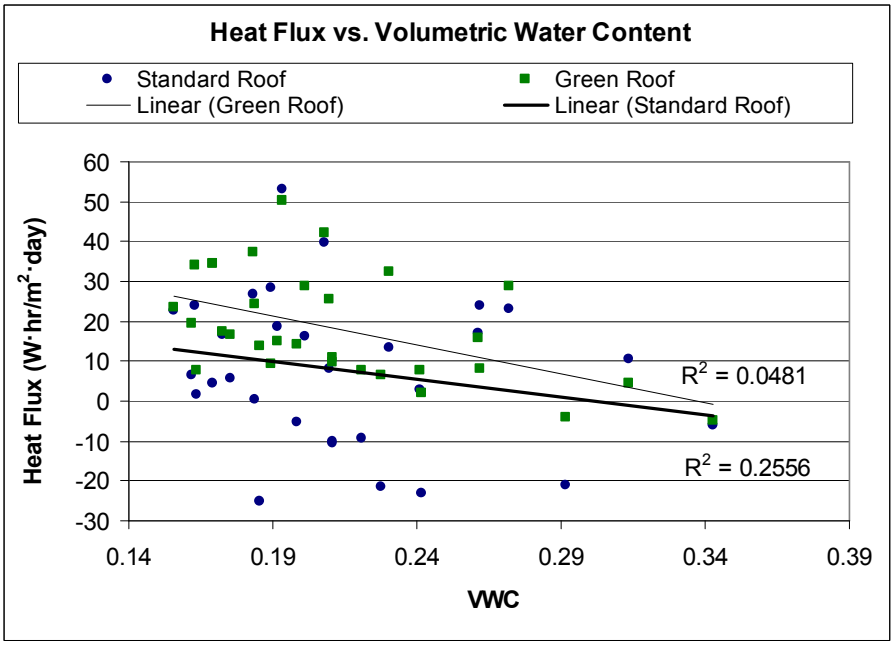

Figure **3.31**: Heat Flux vs. Volumetric Water Content.

It is not expected that the heat flux would depend heavily on the soil moisture for the standard roof, but some dependence should be present for the green roof, as evapotranspiration and soil reflectivity depends on the water content. Heat flux depends on many more variables throughout the month, such as wind speed and under membrane temperature. Plotting heat flux vs. Volumetric Water Content, this speculation is validated, as it is apparent that there does not seem to be much of a trend for either the standard roof or the green roof. However, the correlation coefficient values can be obtained and analyzed. For the green roof, $R^2 = 0.2556$, whereas, for the Standard Roof, $R^2 = 0.0481$. The green roof has a higher correlation coefficient since the heat flux for the green roof does depend in part on the Volumetric Water Content. As the standard roof has no soil, the heat flux does not at all depend on the Volumetric Water Content.

Chapter 4

Conclusions and Future Work

5.1 Conclusions

By analyzing Volumetric Water Content and precipitation, solar radiation and roof top wind speed, under membrane temperature for standard and green roofs, heat flux and solar radiation for standard and green roofs, and heat flux vs. Volumetric Water Content, many observations can be made. For most of these variables, the data and plots show certain trends that occur throughout the month. Other variables reveal more information regarding the performance of the green roof as compared with the white reflective standard roof. Based on these analyses, the main findings of this thesis relate to: (1) the lower variation of the under membrane temperature for the green roof, (2) the total daily incoming heat flux increase of the green roof, and (3) the heat flux peak reduction of the green roof. Each of these points may be expanded and summarized.

First of all, as found in section 3.2.3, the under membrane temperature variation from day to night of the standard roof was about 50°F, compared to a variation of 20°F for the green roof. The decrease of variation for the green roof is significant because there will be less stress on the water proof membrane due to thermal expansion and contraction. Secondly, the standard roof performed better in terms of heat flux, as discussed in section 3.2.4, with a savings of 309 $W \cdot hr/m^2 \cdot month$. However, although these savings are significant, there are other measures of performance that must be considered. This leads to the third finding. The plots of heat flux

show that the soil and plants on green roofs indeed damp the oscillations and reduce the peak heat flux. Consequently, this may result in energy savings due to the decreased necessity of running an air conditioner as much as would be necessary with the higher peak heat flux of the standard roof. The peak heat flux was reduced by 2 W/m^2 to 6 W/m^2.

Finally, as the data for the roof in Chicago compared the white reflective roof with a green roof, the differences in the performance of these two roofs may be explained a bit further. Both have their strengths and weaknesses. The net radiation of the green roof was about four times as great as that of the white reflective roof. This is due to the fact that the reflectivity, ρ, of the reflective roof is four times as large as that of the green roof, and the net radiation and daily incoming heat flux are dependent on this value of reflectivity. However, the green roof reduced peak energy savings, again, due to the evapotranspiration of the soil and plants. The soil and plants of the green roof play a large role in reducing runoff as well. Although not directly proven through the analyses in this thesis, green roofs have benefits with regard to drainage, as described in section 3.2.1, with the analysis of Volumetric Water Content, and it can be inferred from this data that there was no runoff on the green roof in Chicago for the month of July.

5.2 Future Work

The weather station designed in Chapter 1 of this thesis will be used by future students conducting research under Dr. Srebric, as it will be implemented on the Forest Resource Building green roof on the Pennsylvania State University's campus. This weather station will collect data, not unlike the data collected from the roof in Chicago. This data can then be analyzed and used in the heat and mass transfer model. Additionally, the data analyzed for the

roof in Chicago will be studied further and used to validate and refine the heat and mass transfer model. Finally, perhaps data from another study similar to that for the roof in Chicago may offer a comparison between a green roof and a standard black roof.

Furthermore, it is important to note that plants play a large role in the performance of green roofs, significantly reducing the heat flux and runoff, among other advantages. However, plants can be unstable; erosion, drought, and other environmental processes can prevent plants from effectively fulfilling their role on a green roof. Once the properties of the plants and the characteristics of a green roof are determined, it is possible to investigate utilizing an existing material or developing a new organic-inorganic material that may serve the same purpose of plants on a green roof. This material would hopefully be more stable and possibly even more effective than plants. In reality, the future opportunities to develop this technology are great.

Appendix

Figures 3.32-3.35 show the original weekly plots for Volumetric Water Content and Precipitation before the data was corrected for calibration error. Refer to section 3.2.1.

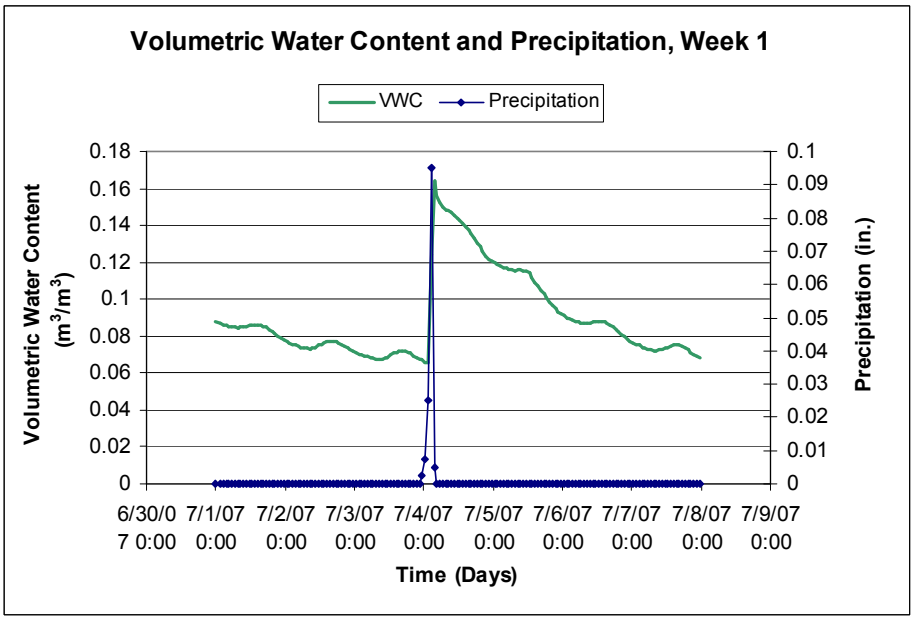

Figure **3.32**: Volumetric Water Content and Precipitation, Week 1.

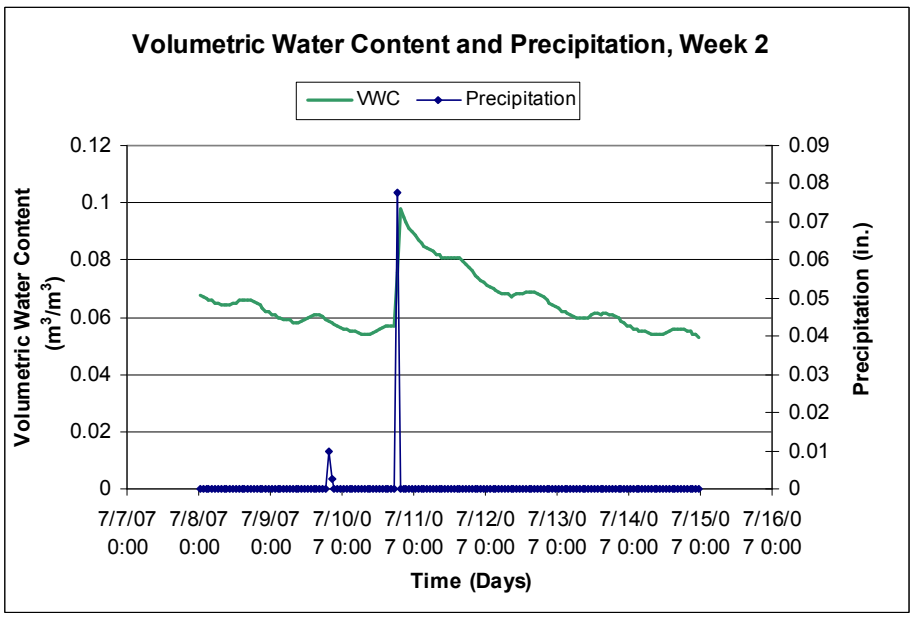

Figure **3.33**: Volumetric Water Content and Precipitation, Week 2.

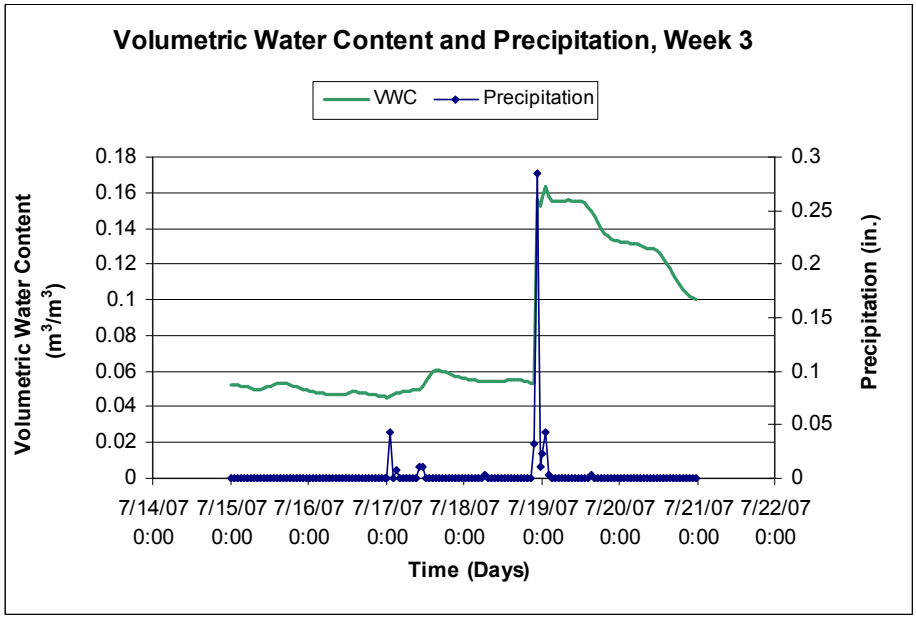

Figure **3.34**: Volumetric Water Content and Precipitation, Week 3.

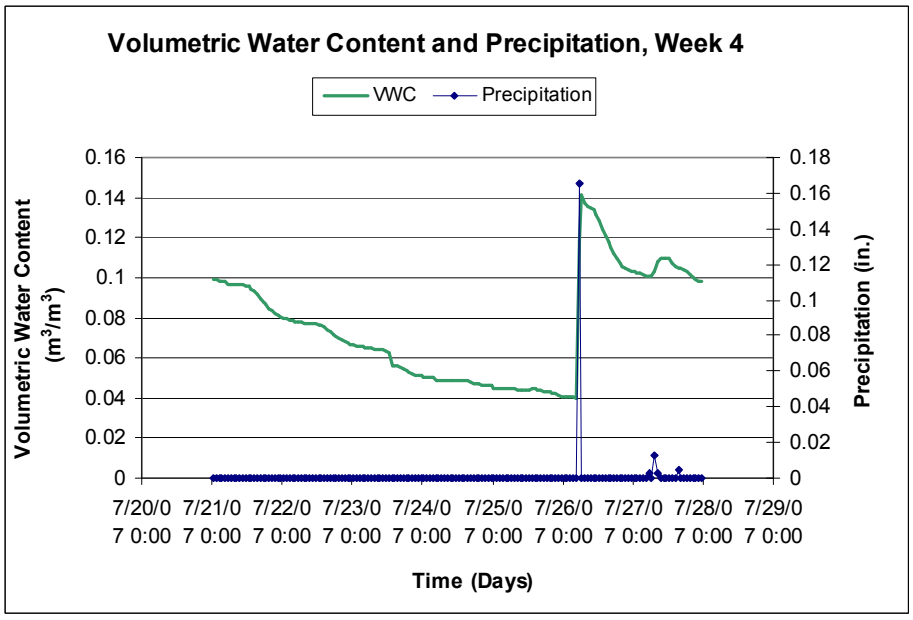

Figure **3.35**: Volumetric Water Content and Precipitation, Week 4.

References

1. Cengel, Y.A., 2006. *Heat and Mass Transfer: A Practical Approach*. New York: McGraw-Hill.

2. Cambell Scientific, 2009a. CS616 and CS625 Water Content Reflectometers Instruction Manual 2002-2004. Accessed on 09 Nov. 2009 <http://www.campbellsci.com/cs616-l>.

3. Campbell Scientific, 2009b. Accessed on 09 Nov. 2009 <http://www.campbellsci.com/hfp01>.

4. Duffie, J.A. and Beckman, W.A., 1991. *Solar Engineering of Thermal Processes*. Hoboken: John Wiley & Sons.

5. Gaffin, S., Rosenzweig, C., Parshall, L., Beattie, D., Berghage, R., O'Keeffe, G., and Braman, D., 2005. "Energy Balance Modeling Applied to a Comparison of White and Green Roof Cooling Efficiency." *Greening Rooftops for Sustainable Communities*. Washington, D.C. May 4-6.

6. Incropera, F.P., DeWitt, D.P., Bergman, T.L., and Levine, A.S., 2007. *Fundamentals of Heat and Mass Transfer*. Hoboken: John Wiley & Sons.

7. International Thermal Instrument Company, 2008. Accessed on 09 Nov. 2009 <http://iticompany.com/pages/instruments/02/index.htm>.

8. Liu, K.K.Y., 2004. "Sustainable building envelope – garden roof system performance." *RCI Building Envelope Symposium*. New Orleans, LA. April 11.

9. MicroDAQ, 2009. TheDataLoggerStore.com. Accessed on 10 Sept. 2009 <http://www.microdaq.com>.

10. Tabares-Velasco, P.C., 2009. "Predictive Heat and Mass Transfer Model of Plant-Based Roofing Materials for Assessment of Energy Savings." Ph.D. Thesis, Department of Architectural Engineering, the Pennsylvania State University, State College, PA.

11. Tabares-Velasco, P.C. and Srebric, J., 2009a. "Heat Fluxes and Water Management of a Green and Brown Roof: Laboratory Experiments." *Greening Rooftops for Sustainable Communities conference, awards, and trade show*. Atlanta, GA. June 1-9.

12. Tabares-Velasco, P.C. and Srebric, J., 2009b. "Predictive Green Roof Model for Assessment of Heat and Mass Transfer through a Roof Assembly in Summer Weather Conditions." In preparation for the *International Journal of Heat and Mass Transfer*.

13. Tabares-Velasco, P.C. and Srebric, J., 2009c. "The Role of Plants in the Reduction of Heat Flux through Green Roofs: Laboratory Experiments." *ASHRAE Transactions*.

Academic Vita

NICOLE L. PETERSON
nlp130@psu.edu

EDUCATION:
The Pennsylvania State University, University Park, PA
Schreyer Honors College
B.S. in Mechanical Engineering
B.S. in Spanish
B.S. in International Studies

Honors: Mechanical Engineering
Thesis Title: On-site Performance of Extensive Green Roofs
Thesis Supervisor: Dr. Jelena Srebric

WORK EXPERIENCE:
Applied Science Building, Penn State University, Spring 2007
Research assistant in Marine Bioacoustics
-Assisted Dr. Susan E. Parks with her research on North Atlantic right whales.
-Analyzed the spectrograms for various whale calls.
-Focused on mother-offspring communication and the idea of sharing "acoustic space."

AWARDS:
Recipient of the Howard J. Waltemeyer, Sr. Scholarship from the College of Engineering (2008-09 and 2009-10 academic years)
Recipient of the John W. White Scholarship for Excellence in Spanish from the College of Spanish, Italian, and Portuguese (Spring 2008)
Recipient of the Paul Morrow Endowed Scholarship from the College of Engineering (2006-07 and 2007-08 academic years)

PROFESSIONAL MEMBERSHIPS:
American Society of Mechanical Engineers (ASME), Fall 2008-present
Society of Women Engineers (SWE), Fall 2005-present

VOLUNTEER EXPERIENCE:
A.P.E.M.A., Buenos Aires, Argentina, Spring 2008
-Volunteered at this non-profit association for the protection of animals during my stay in Buenos Aires.
-Was in support of more laws for animal rights in Argentina.

ACTIVITIES:
Driver in Shell's Eco-Marathon Americas, Spring 2009
Participant in ASME Rube Goldberg Competition, Spring 2009
Active member and officer of PSU Photography Club, Fall 2005-present
Active member of PSU Tennis Club, Fall 2005-present
Coxswain for the Penn State Crew Team, Spring 2006

SKILLS:
Language Skills: Fluent in Spanish, studied abroad in Argentina in Spring 2008
Computer Skills: Microsoft Office, Matlab, SolidWorks (CSWA certified)